IPAS-HEP-k006
KEK-TH-714
Dec 2000
ed. Mar 2001

One-loop Neutron Electric Dipole Moment from Supersymmetry without R parity

Y.-Y. Keum[1] * **and Otto C. W. Kong**[1,2] †

[1]*Institute of Physics, Academia Sinica, Nankang, Taipei, Taiwan 11529*

[2]*Theory Group, KEK, Tsukuba, Ibaraki, 305-0801, Japan*

Abstract

We present a detailed analysis together with exact numerical calculations on one-loop contributions to the neutron electric dipole moment from supersymmetry without R parity, focusing on the gluino, chargino, and neutralino contributions. Apart from the neglected family mixing among quarks, complete formulae are given for the various contributions through the quark dipole operators, to which the present study is restricted. We discuss the structure and main features of the R-parity violating contributions and the interplay between the R-parity conserving and violating parameters. In particular, the parameter combination $\mu_i^* \lambda'_{i11}$, under the optimal parametrization adopted, is shown to be solely responsible for the R-parity violating contributions in the supersymmetric loop diagrams. While $\mu_i^* \lambda'_{i11}$ could bear a complex phase, the latter is not necessary to have a R-parity violating contribution.

PACS index: 13.40.Em,11.30.Er,12.60.Jv,14.80.Ly

*E-mail: keum@phys.sinica.edu.tw

†E-mail: kongcw@phys.sinica.edu.tw

I. INTRODUCTION

Neutron and electron electric dipole moments (EDMs) are important topics for new CP violating physics. They are known to be extremely small in the Standard Model (SM); in fact, way below the present experimental limit. With supersymmetry (SUSY) comes many plausible extra EDM contributions. That has led to the so-called SUSY CP problem [1] for the minimal supersymmetric standard model (MSSM). If one simply takes the minimal supersymmetric spectrum of the SM and imposes nothing more than the gauge symmetries while still admitting soft SUSY breaking, the generic supersymmetric standard model would result. When the large number of baryon and/or lepton number violating terms in such a generic supersymmetric SM are removed by hand, through imposing an *ad hoc* discrete symmetry called R parity, one obtains the MSSM Lagrangian. In the case of R-parity violation, two recent papers focus on the contributions from the extra trilinear terms in the superpotential and conclude that there is no new EDM contribution at the 1-loop level [2]. Perhaps it has not been emphasized enough in the two papers that they are *not* studying the complete theory of SUSY without R parity, which is nothing other than the generic supersymmetric SM; in particular, they have nelgected admissible RPV parameters other than the trilinear ones in the superpotential. It is interesting to see that in the generic case there are in fact contributions at the 1-loop level, as pointed out in Refs. [3,4]. In particular, Ref. [3] gives a clear illustration of the much overlooked existence of a R-parity violating (RPV) contribution to LR squark mixings and the resulting contribution to neutron EDM through the simple 1-loop gluino diagram. We would like to emphasize again that the new contribution involves both bilinear and trilinear (RPV) couplings in the superpotential. Since RPV scenarios studied in the literature typically admit only one of the two types of couplings, the contribution has not been previously identified. A simple estimate of the bound obtained on the RPV parameters (the $\mu_i^* \lambda'_{i11}$ combination) given in Ref. [3] has already illustrated that the bound from the neutron EDM as one of the most important, being competitive even when compared with sub-eV neutrino mass bounds and substantially more stringent than most collider bounds. The present article aims at giving a detailed analysis and numerical study of the RPV extension of SUSY contributions to neutron EDM. Similar new RPV contributions to electron EDM have been noted in Ref. [3]. In fact, the complete result for RPV contributions to the masses of the sleptons and other (color-singlet) scalars has been given in Ref. [5], which focuses mainly on their implications to neutrino masses.

The complete theory of SUSY without R parity admits all kinds of RPV terms without bias. It is obviously better motivated than *ad hoc* versions of RPV theories. The large number of new parameters involved, however, makes the theory difficult to analyze. The question of the specification of flavor bases to define the parameters in the Lagrangian of

the theory unambiguously becomes more important. In fact, thinking about the theory as the generic supersymmetric SM instead of as "MSSM + RPV terms" helps to clarify many of the issues involved [6]. From such a perspective, it has been illustrated [7] that an optimal parametrization, called the single-VEV parametrization (SVP), provides a very nice formulation which helps to simplify much of the analysis. In particular, the SVP gives the complete results for the tree-level mass matrices of all state, fermions as well as scalars, in the simplest form [5]. The formulation has been used to study leptonic phenomenology [7] and various aspects of neutrino masses [5,8–11]. The present EDM study (also Refs. [3,4]) and parallel works on $\mu \to e\,\gamma$ [12] (see also Ref. [13]), electron EDM, and $b \to s\,\gamma$ [14] will further illustrate the advantage of adopting the SVP.

We focus here only on such contributions to the neutron EDM, based on the valence quark model [15]. Hence, we study only the 1-loop quark EDMs. We will give complete 1-loop formulae for EDMs of the up- and down-sector quarks, of which the u and d results are used to calculate the neutron EDM through the

$$d_n = \frac{1}{3}\,(4\,d_d - d_u)\;\eta \tag{1}$$

formula, where $\eta \simeq 1.53$ is a QCD correction factor from renormalization group evolution [16,17]. This is to be matched with the experimental bound [18]

$$d_n < 6.3 \cdot 10^{-26}\, e \cdot \mathrm{cm}\ .$$

In the MSSM case, one has the SUSY loop contributions and the charged Higgs contributions. The latter are very negligible. We focus here in this article on the analogue of the 1-loop SUSY contributions. The latter include the gluino loop, the charginolike loop, and the neutralinolike loop. By the last two, we mean generalization of the chargino and neutralino loops under the generic picture. The (RPV) mixings of the leptons with the gauginos and Higgsinos give five (color-singlet) charged leptons and seven neutral fermions, including the charginos and neutralinos as well as e, μ, τ, and three physical neutrinos. They come from the same set of electroweak states and should not be separated from one another in the analysis. It is no surprise that the physical chargino and neutralino states dominate the EDM contributions. We use explicit exact mass eigenstate expressions in our analysis to illustrate that as well as other interesting features, starting from the generic electroweak states couplings under the SVP. An exact numerical calculation is performed. We would like to mention that the generalization of the charged Higgs loop contribution involves other different RPV parameters. Moreover, there are many new and potentially important contributions including a t-quark loop, as also pointed out in Ref. [4]. We will give also the formulae of such quark-scalar loop contributions, though a detailed study is postponed to a future publication. Note that Ref. [4], which first appeared around the same time as Ref. [3], is the only other study of the same topic available. In our opinion, our study here is

more systematic and complete. Ref. [4] does not include, for example, the RPV LR scalar mixing and the resulted gaugino loop contribution to EDM. Moreover, to the best of our knowlegde, the present study includes the first exact numerical calculation performed. Ref. [4] also quotes a $\cos\beta$ dependence of the major charginolike contribution, hence a weakening of the bound in the large $\tan\beta$ regime — a result with which we disagree. Our careful numerical study illustrates many more interesting features, as the discussion below will speak for itself.

This paper is organized as follows: We first summarize the formulation and notation used in Sec. II, where we also elaborate in some detail on the electroweak fermion field couplings needed to study the quark EDMs. Next, Sec. III contains results presented recently in Ref. [5] on all the scalar masses, listed here so that the present paper will be self-contained. Of most importance here is the RPV contributions to LR mixings, which play a central part in the EDM contributions. The quark EDMs are analyzed in Sec. IV. Some results from our numerical calculations are presented in Sec. V, after which we conclude in Sec. VI. An appendix gives some background formulae on the color-singlet fermion masses. Note that our formulae and calculations here naturally include the R-parity conserving MSSM part, though we will concentrate on the role of the RPV parameters and their unique contributions. Corresponding studies of the MSSM case can be found, for example, in Refs. [16,19–21], to which we refer the readers for comparison.

II. FORMULATION AND NOTATION

We summarize our formulation and notation below. The most general renormalizable superpotential for the generic supersymmetric SM can be written then as

$$W = \varepsilon_{ab}\left[\mu_\alpha \hat{H}_u^a \hat{L}_\alpha^b + y_{ik}^u \hat{Q}_i^a \hat{H}_u^b \hat{U}_k^C + \lambda'_{\alpha jk}\hat{L}_\alpha^a \hat{Q}_j^b \hat{D}_k^C + \frac{1}{2}\,\lambda_{\alpha\beta k}\hat{L}_\alpha^a \hat{L}_\beta^b \hat{E}_k^C\right] + \frac{1}{2}\,\lambda''_{ijk}\hat{U}_i^C \hat{D}_j^C \hat{D}_k^C \ , \quad (2)$$

where (a,b) are $SU(2)$ indices, (i,j,k) are the usual family (flavor) indices, and (α,β) are the extended flavor indices going from 0 to 3. At the limit where $\lambda_{ijk}, \lambda'_{ijk}, \lambda''_{ijk}$, and μ_i all vanish, one recovers the expression for the R-parity preserving case (*i.e.,* MSSM), with $\hat{L}_0$ identified as $\hat{H}_d$. Without R parity imposed, the latter is not *a priori* distinguishable from the $\hat{L}_i$'s. Note that λ is antisymmetric in the first two indices, as required by the $SU(2)$ product rules, as shown explicitly here with $\varepsilon_{12} = -\varepsilon_{21} = 1$. Similarly, λ'' is antisymmetric in the last two indices from $SU(3)_C$.

R parity is exactly an *ad hoc* symmetry put in to make $\hat{L}_0$ stand out from the other $\hat{L}_i$'s as the candidate for $\hat{H}_d$. It is defined in terms of baryon number, lepton number, and spin as, explicitly, $\mathcal{R} = (-1)^{3B+L+2S}$. The consequence is that the accidental symmetries of baryon number and lepton number in the SM are preserved, at the expense of making

particles and superparticles having a categorically different quantum number, R parity. The latter is actually not the most effective discrete symmetry to control superparticle mediated proton decay [22], but is most restrictive in terms of what is admitted in the Lagrangian, or the superpotential alone.

A naive look at the scenario suggests that the large number of new couplings makes the task formidable. However, it becomes quite manageable with an optimal choice of flavor bases, the SVP [7]. In fact, doing phenomenological studies without specifying a choice of flavor bases is ambiguous. It is like doing SM quark physics with 18 complex Yukawa couplings instead of the 10 real physical parameters. For SUSY without R parity, the choice of an optimal parametrization mainly concerns the 4 $\hat{L}_\alpha$ flavors. Under the SVP [1] , flavor bases are chosen such that 1/ among the $\hat{L}_\alpha$'s, only $\hat{L}_0$, bears a VEV (*i.e.,* $\langle \hat{L}_i \rangle \equiv 0$); 2/ $y^e_{jk} (\equiv \lambda_{0jk} = -\lambda_{j0k}) = \frac{\sqrt{2}}{v_0} \, \mathrm{diag}\{m_1, m_2, m_3\}$; 3/ $y^d_{jk} (\equiv \lambda'_{0jk}) = \frac{\sqrt{2}}{v_0} \, \mathrm{diag}\{m_d, m_s, m_b\}$; 4/ $y^u_{ik} = \frac{\sqrt{2}}{v_u} \, V^T_{\rm CKM} \, \mathrm{diag}\{m_u, m_c, m_t\}$, where $v_0 \equiv \sqrt{2} \, \langle \hat{L}_0 \rangle$ and $v_u \equiv \sqrt{2} \, \langle \hat{H}_u \rangle$. The big advantage of here is that the (tree-level) mass matrices for all the fermions do not involve any of the trilinear RPV couplings, though the approach makes no assumption on any RPV coupling including even those from soft SUSY breaking, and all the parameters used are uniquely defined, with the exception of some removable phases.

We are interested in scalar-fermion-fermion couplings similar to those of the charginos and neutralinos in the MSSM. The gaugino couplings are, of course, standard. Coming from the gauge interaction parts, they have nothing to do with R parity. The "Higgsino-like" part is, however, different. Without R parity and in a generic flavor basis of the four $\hat{L}_\alpha$'s, the $\hat{H}_d$ of the MSSM is hidden among the latter. The SVP, however, identifies $\hat{L}_0$ as the one having "Higgs" properties of $\hat{H}_d$, though it still maintains (RPV) couplings similar to those of the $\hat{L}_i$'s. We write the components of a $\hat{L}_\alpha$ fermion doublet as l^0_α and l^-_α, and their scalar partners as $\tilde{l}^0_\alpha$ and $\tilde{l}^-_\alpha$. Apart from being better motivated theoretically, the common notation helps to trace the flavor structure. However, we will also use notation of the form $h^\star_d$ and $\tilde{h}^\star_d$ as alternative notation for $\tilde{l}^\star_0$ and $l^\star_0$ in some places below. This is unambiguous under our formulation. We will also referred to $h^\star_d$ and $\tilde{h}^\star_d$ as the Higgs boson and Higgsino, respectively, while they are generally also included in the terms slepton and lepton.

Note that in the left-handed lepton and slepton field notation introduced above, we have dropped the commonly used L subscript, for simplicity. For the components of the three right-handed leptonic superfields, we use l^+_i and $\tilde{l}^+_i$, with again the R subscript dropped. The notation for the quark and squark fields will be standard, with the L and R subscripts.

---

[1] Note that our notation here is a bit different from that in Ref. [7]; we follow mostly the notation in Refs. [3] and [5] while improving and elaborating further whenever appropriate. We will clarify all notation used as our discussion goes along [6].

A normal quark state, such as d_{L_k}, denotes a mass eigenstate, while a squark state the supersymmetric partner of one. A quark or squark state with a $\prime$ denotes one with the quark state being the $SU(2)$ partner of a mass eigenstate. For instance, $\tilde{u}'_{L_3}$ is the up-type squark state from $\hat{Q}_3$ which contains the exact left-handed b quark according to our parametrization of the Lagrangian.

The up-sector Higgs boson is unaffected by R-parity violation. The scalar and fermion states of the doublet are denoted by h_u^+, h_u^0 and $\tilde{h}_u^+$, $\tilde{h}_u^0$, respectively.

The identity of the charginos and neutralinos is unambiguous in the MSSM. Without R parity, they mix with the charged leptons and neutrinos. In fact, the true charged leptons and neutrinos are the light mass eigenstates of the full 5×5 and 7×7 mass matrices, respectively. The mass eigenstates deviate from the l_i^-'s and l_i^0's. Though the latter deviations are practically negligible in the limit of small μ_i's, it still helps to distinguish the electroweak states from the mass eigenstates. Moreover, large R-parity violation, especially in terms of a large μ_3, is not definitely ruled out [7]. Here, in this paper, we make the explicit distinction and reserve the terms chargino and neutralino for the heavy states beyond the physical charged leptons e, μ, and τ and neutrinos. The m_i's introduced above are the Yukawa contributions to the physical charged lepton masses, hence approximately equal to the latter. The readers are referred to the appendix for more details about the fermion mass terms.

We are now ready to spell out the couplings concerning the (color-singlet) charged and neutral fermions from the superpotential. We have

$$\begin{aligned}\mathcal{L}_\chi = {} & y_{u_i}\, V_{\rm CKM}^{ij}\, \tilde{h}_u^+ \left[\, \tilde{u}^c_{R_i}\, d_{L_j} + u^c_{R_i}\, \tilde{d}_{L_j} \,\right] + y_{d_i}\, l_0^- \left[\, \tilde{d}^c_{R_i}\, u'_{L_i} + d^c_{R_i}\, \tilde{u}'_{L_i} \,\right] + \lambda'_{ijk}\, l_i^- \left[\, \tilde{d}^c_{R_k}\, u'_{L_j} + d^c_{R_k}\, \tilde{u}'_{L_j} \,\right] \\ & - y_{u_i}\, \tilde{h}_u^0 \left[\, \tilde{u}^c_{R_i}\, u_{L_i} + u^c_{R_i}\, \tilde{u}_{L_i} \,\right] - y_{d_i}\, l_0^0 \left[\, \tilde{d}^c_{R_i}\, d_{L_i} + d^c_{R_i}\, \tilde{d}_{L_i} \,\right] - \lambda'_{ijk}\, l_i^0 \left[\, \tilde{d}^c_{R_k}\, d_{L_j} + d^c_{R_k}\, \tilde{d}_{L_j} \,\right] \\ & + y_{e_i} \left[\, l_0^-\, l_i^+\, \tilde{l}_i^0 \, - l_i^-\, l_i^+\, \tilde{l}_0^0 \,\right] + y_{e_i} \left[\, l_0^-\, l_i^0\, \tilde{l}_i^+ \, - l_i^-\, l_0^0\, \tilde{l}_i^+ \,\right] + y_{e_i} \left[\, l_i^0\, l_i^+\, \tilde{l}_0^- \, - l_0^0\, l_i^+\, \tilde{l}_i^- \,\right] \\ & + \lambda_{ijk}\, l_i^-\, l_k^+\, \tilde{l}_j^0 + \lambda_{ijk}\, l_i^-\, l_j^0\, \tilde{l}_k^+ - \lambda_{ijk}\, l_i^0\, l_k^+\, \tilde{l}_j^- \quad + \quad \text{h.c.} \ , \end{aligned} \tag{3}$$

where

$$y_{u_i} = \frac{g_2\, m_{u_i}}{\sqrt{2}\, M_W\, \sin\beta} \ , \qquad y_{d_i} = \frac{g_2\, m_{d_i}}{\sqrt{2}\, M_W\, \cos\beta} \ , \qquad y_{e_i} = \frac{g_2\, m_i}{\sqrt{2}\, M_W\, \cos\beta} \tag{4}$$

are the (diagonal) quark and charged lepton Yukawa couplings, and $\tan\beta = \frac{v_u}{v_0}$ [23]. Recall that λ'_{0jk} corresponds to the down-quark Yukawa coupling matrix, and λ_{0jk} corresponds to the charged lepton Yukawa coupling matrix, both of which are diagonal under the SVP; in addition, we have $u'_{L_i} = V_{\rm CKM}^{\dagger\, ij}\, u_{L_j}$ being the $SU(2)$ partner of the mass eigenstate d_{L_i}, and $\tilde{u}'_{L_i}$ its scalar partner. We also use below $\tilde{d}'_{L_i}$, which is, explicitly, $V_{\rm CKM}^{ij}\, \tilde{d}_{L_j}$. There are some more scalar-fermion-fermion terms besides those given in $\mathcal{L}_\chi$. These extra terms are slepton-quark-quark terms. We will see that the latter are actually also involved in 1-loop EDM diagrams, though not the major focus of this paper. With the above explicit listed terms, however, it is straightforward to see what the extra terms are like.

In both of the above expressions for $\mathcal{L}_\chi$, there is a clear distinction between the MSSM terms and the RPV terms. The nice feature is a consequence of the SVP. The simple structure of the trilinear coupling contributions to the d-quark and charged lepton masses, which is equivalent to that of the R-parity conserving limit, is what makes the analysis simple and easy to handle. We want to emphasize that the above expressions are exact tree-level results without hidden assumptions behind their validity. They are good even when there is large R-parity violation.

III. SQUARK AND SLEPTON MASSES

The soft SUSY breaking part of the Lagrangian, in terms of scalar parts of the superfield multiplets, can be written as follows:

$$\begin{aligned} V_{\rm soft} &= \epsilon_{ab} B_\alpha \, H_u^a \tilde{L}_\alpha^b + \epsilon_{ab} \left[\, A_{ij}^{U} \, \tilde{Q}_i^a H_u^b \tilde{U}_j^C + A_{ij}^{D} H_d^a \tilde{Q}_i^b \tilde{D}_j^C + A_{ij}^{E} H_d^a \tilde{L}_i^b \tilde{E}_j^C \, \right] + \text{h.c.} \\ &+ \epsilon_{ab} \left[\, A_{ijk}^{\lambda'} \tilde{L}_i^a \tilde{Q}_j^b \tilde{D}_k^C + \frac{1}{2} \, A_{ijk}^{\lambda} \tilde{L}_i^a \tilde{L}_j^b \tilde{E}_k^C \right] + \frac{1}{2} \, A_{ijk}^{\lambda''} \tilde{U}_i^C \tilde{D}_j^C \tilde{D}_k^C + \text{h.c.} \\ &+ \tilde{Q}^\dagger \tilde{m}_{Q}^2 \, \tilde{Q} + \tilde{U}^\dagger \tilde{m}_{U}^2 \, \tilde{U} + \tilde{D}^\dagger \tilde{m}_{D}^2 \, \tilde{D} + \tilde{L}^\dagger \tilde{m}_{L}^2 \tilde{L} + \tilde{E}^\dagger \tilde{m}_{E}^2 \, \tilde{E} + \tilde{m}_{H_u}^2 \, |H_u|^2 \\ &+ \frac{M_1}{2} \tilde{B}\tilde{B} + \frac{M_2}{2} \tilde{W}\tilde{W} + \frac{M_3}{2} \tilde{g}\tilde{g} + \text{h.c.} \, , \end{aligned} \tag{5}$$

where we have separated the R-parity conserving ones from the RPV ones ($H_d \equiv \tilde{L}_0$) for the A terms. Note that $\tilde{L}^\dagger \tilde{m}_{\tilde{L}}^2 \tilde{L}$, unlike the other soft mass terms, is given by a 4×4 matrix. Explicitly, $\tilde{m}_{L_{00}}^2$ is $\tilde{m}_{H_d}^2$ of the MSSM case while $\tilde{m}_{L_{0k}}^2$'s give RPV mass mixings. The other notation is obvious.

The SVP also simplifies much the otherwise extremely complicated expressions for the mass-squared matrices of the scalar sectors. First, we will look at the squarks sectors. The masses of up squarks obviously have no RPV contribution. The down-squark sector, however, has an interesting result. We have the mass-squared matrix as follows:

$$\mathcal{M}_{D}^2 = \begin{pmatrix} \mathcal{M}_{LL}^2 & \mathcal{M}_{RL}^{2\dagger} \\ \mathcal{M}_{RL}^2 & \mathcal{M}_{RR}^2 \end{pmatrix} \, , \tag{6}$$

where

$$\begin{aligned} \mathcal{M}_{LL}^2 &= \tilde{m}_{Q}^2 + m_{D}^\dagger m_{D} + M_Z^2 \, \cos 2\beta \left[-\frac{1}{2} + \frac{1}{3} \sin^2 \theta_W \right] \, , \\ \mathcal{M}_{RR}^2 &= \tilde{m}_{D}^2 + m_{D} m_{D}^\dagger + M_Z^2 \, \cos 2\beta \left[-\frac{1}{3} \sin^2 \theta_W \right] \, , \end{aligned} \tag{7}$$

and

$$\begin{aligned} (\mathcal{M}_{RL}^2)^T &= A^{D} \frac{v_0}{\sqrt{2}} - (\, \mu_\alpha^* \lambda'_{\alpha jk} \,) \, \frac{v_u}{\sqrt{2}} \\ &= [A_d - \mu_0^* \, \tan\beta] \, m_{D} \, + \frac{\sqrt{2} \, M_W \cos\beta}{g_2} \, \delta A^{D} - \frac{\sqrt{2} \, M_W \sin\beta}{g_2} \, (\, \mu_i^* \lambda'_{ijk} \,) \, . \end{aligned} \tag{8}$$

Here, $m_{\scriptscriptstyle D}$ is the down-quark mass matrix, which is diagonal under the parametrization adopted; A_d is a constant (mass) parameter representing the "proportional" part of the A term and the matrix $\delta A^{\scriptscriptstyle D}$ is the "proportionality" violating part; $(\,\mu_i^*\lambda'_{ijk}\,)$, and similarly $(\,\mu_\alpha^*\lambda'_{\alpha jk}\,)$, denotes the 3×3 matrix $(\ )_{jk}$ with elements listed [2] . The $(\,\mu_\alpha^*\lambda'_{\alpha jk}\,)$ term is the full F-term contribution, while the $(\,\mu_i^*\lambda'_{ijk}\,)$ part separated out in the last expression gives the RPV contributions.

Next we go on to the slepton sector. From Eq.(5) above, we can see that the charged Higgs bosons should be considered on the same footing together with the sleptons. We have hence an 8×8 mass-squared matrix of the following $1+4+3$ form:

$$\mathcal{M}_{\scriptscriptstyle E}^2 = \begin{pmatrix} \widetilde{\mathcal{M}}^2_{\scriptscriptstyle Hu} & \widetilde{\mathcal{M}}^{2\dagger}_{\scriptscriptstyle LH} & \widetilde{\mathcal{M}}^{2\dagger}_{\scriptscriptstyle RH} \\ \widetilde{\mathcal{M}}^2_{\scriptscriptstyle LH} & \widetilde{\mathcal{M}}^2_{\scriptscriptstyle LL} & \widetilde{\mathcal{M}}^{2\dagger}_{\scriptscriptstyle RL} \\ \widetilde{\mathcal{M}}^2_{\scriptscriptstyle RH} & \widetilde{\mathcal{M}}^2_{\scriptscriptstyle RL} & \widetilde{\mathcal{M}}^2_{\scriptscriptstyle RR} \end{pmatrix} , \tag{9}$$

where

$$\begin{aligned} \widetilde{\mathcal{M}}^2_{\scriptscriptstyle Hu} &= \tilde{m}^2_{\scriptscriptstyle Hu} + \mu_\alpha^*\mu_\alpha + M_{\scriptscriptstyle Z}^2\,\cos2\beta\left[\frac{1}{2} - \sin^2\theta_{\scriptscriptstyle W}\right] \\ &\quad + M_{\scriptscriptstyle Z}^2\,\sin^2\beta\,[1-\sin^2\theta_{\scriptscriptstyle W}]\,, \\ \widetilde{\mathcal{M}}^2_{\scriptscriptstyle LL} &= \tilde{m}^2_{\scriptscriptstyle L} + m_{\scriptscriptstyle L}^\dagger m_{\scriptscriptstyle L} + (\mu_\alpha^*\mu_\beta) + M_{\scriptscriptstyle Z}^2\,\cos2\beta\left[-\frac{1}{2} + \sin^2\theta_{\scriptscriptstyle W}\right] \\ &\quad + \begin{pmatrix} M_{\scriptscriptstyle Z}^2\,\cos^2\beta\,[1-\sin^2\theta_{\scriptscriptstyle W}] & 0_{1\times3} \\ 0_{3\times1} & 0_{3\times3} \end{pmatrix}, \\ \widetilde{\mathcal{M}}^2_{\scriptscriptstyle RR} &= \tilde{m}^2_{\scriptscriptstyle E} + m_{\scriptscriptstyle E} m_{\scriptscriptstyle E}^\dagger + M_{\scriptscriptstyle Z}^2\,\cos2\beta\left[-\sin^2\theta_{\scriptscriptstyle W}\right]\,, \end{aligned} \tag{10}$$

and

$$\begin{aligned} \widetilde{\mathcal{M}}^2_{\scriptscriptstyle LH} &= (B_\alpha^*) + \begin{pmatrix} \frac{1}{2}\,M_{\scriptscriptstyle Z}^2\,\sin2\beta\,[1-\sin^2\theta_{\scriptscriptstyle W}] \\ 0_{3\times1} \end{pmatrix}\,, \\ \widetilde{\mathcal{M}}^2_{\scriptscriptstyle RH} &= -\,(\,\mu_i^*\lambda_{i0k}\,)\,\frac{v_0}{\sqrt{2}} \;=(\,\mu_k^*\,m_k\,) \qquad\qquad \text{(no sum over } k) \quad\,, \\ (\widetilde{\mathcal{M}}^2_{\scriptscriptstyle RL})^{\scriptscriptstyle T} &= \begin{pmatrix} 0 \\ A^{\scriptscriptstyle E} \end{pmatrix}\frac{v_0}{\sqrt{2}} - (\,\mu_\alpha^*\lambda_{\alpha\beta k}\,)\,\frac{v_u}{\sqrt{2}} \\ &= [A_e - \mu_0^*\,\tan\beta]\begin{pmatrix} 0 \\ m_{\scriptscriptstyle E} \end{pmatrix} + \frac{\sqrt{2}\,M_{\scriptscriptstyle W}\cos\beta}{g_2}\begin{pmatrix} 0 \\ \delta A^{\scriptscriptstyle E} \end{pmatrix} - \begin{pmatrix} -\mu_k^*\,m_k\,\tan\beta \\ \frac{\sqrt{2}\,M_{\scriptscriptstyle W}\,\sin\beta}{g_2}\,(\,\mu_i^*\lambda_{ijk}\,) \end{pmatrix}\,. \end{aligned} \tag{11}$$

The notation and results here are similar to the squark case above, with some difference. We have A_e and $\delta A^{\scriptscriptstyle E}$, or the extended matrices $\left(\begin{smallmatrix} 0 \\ \star \end{smallmatrix}\right)$ incorporating them, denoting the splitting of the A term, with proportionality defined with respect to $m_{\scriptscriptstyle E}$; $m_{\scriptscriptstyle L} = \mathrm{diag}\{0, m_{\scriptscriptstyle E}\} =$

[2] Note that we use this kind of bracket notation for matrices extensively here. In this case, the repeated index i is to be summed over as usual and, hence, is dummy.

diag$\{0, m_1, m_2, m_3\}$. Recall that the m_i's are approximately the charged lepton masses. A 4×3 matrix $(\,\mu_i^* \lambda_{i\beta k}\,)$ gives the RPV contributions to $(\widetilde{\mathcal{M}}^2_{RL})^T$. In the above expression, we separate explicitly the first row of the former, which corresponds to mass-squared terms of the type $\tilde{l}^+ h_d^-$ type ($h_d^- \equiv \tilde{l}_0^-$). The nonzero $\widetilde{\mathcal{M}}^2_{RH}$ and the B_i^*'s in $\widetilde{\mathcal{M}}^2_{LH}$ are also RPV contributions. The former is a $\tilde{l}^+ (h_u^+)^\dagger$ type, while the latter a $\tilde{l}^- h_u^+$ term. Note that the parts with the $[1 - \sin^2\theta_W]$ factor are singled out as they are extra contributions to the masses of the charged Higgs bosons (*i.e.,* $l_0^- \equiv h_d^-$ and h_u^+). The latter are the result of quartic terms in the scalar potential and the fact that the Higgs doublets bear VEVs.

The neutral scalar mass terms, in terms of the $(1 + 4)$ complex scalar fields ϕ_n's, can be written in two parts — a simple $(\mathcal{M}^2_{\phi\phi\dagger})_{mn}\, \phi_m^\dagger \phi_n$ part and a Majorana-like part in the form $\frac{1}{2}\,(\mathcal{M}^2_{\phi\phi})_{mn}\, \phi_m \phi_n + \text{h.c.}$ As the neutral scalars originate from chiral doublet superfields, the existence of the Majorana-like part is a direct consequence of the electroweak symmetry breaking VEVs, hence restricted to the scalars playing the Higgs boson role only. They come from the quartic terms of the Higgs fields in the scalar potential. We have, explicitly,

$$\mathcal{M}^2_{\phi\phi} = \frac{1}{2}\, M_Z^2 \begin{pmatrix} \sin^2\beta & -\cos\beta\,\sin\beta & 0_{1\times 3} \\ -\cos\beta\,\sin\beta & \cos^2\beta & 0_{1\times 3} \\ 0_{3\times 1} & 0_{3\times 1} & 0_{3\times 3} \end{pmatrix} , \tag{12}$$

and

$$\mathcal{M}^2_{\phi\phi\dagger} = \mathcal{M}^2_{\phi\phi} + \begin{pmatrix} \tilde{m}^2_{H_u} + \mu_\alpha^* \mu_\alpha + M_Z^2\, \cos 2\beta \left[-\frac{1}{2}\right] & -(B_\alpha) \\ -(B_\alpha^*) & \tilde{m}^2_L + (\mu_\alpha^* \mu_\beta) + M_Z^2\, \cos 2\beta \left[\frac{1}{2}\right] \end{pmatrix} . \tag{13}$$

Note that $\mathcal{M}^2_{\phi\phi}$ here is real (see the Appendix), while $\mathcal{M}^2_{\phi\phi\dagger}$ does have complex entries. The full 10×10 (real and symmetric) mass-squared matrix for the real scalars is then given by

$$\mathcal{M}^2_S = \begin{pmatrix} \mathcal{M}^2_{SS} & \mathcal{M}^2_{SP} \\ (\mathcal{M}^2_{SP})^T & \mathcal{M}^2_{PP} \end{pmatrix} , \tag{14}$$

where the scalar, pseudoscalar, and mixing parts are

$$\begin{aligned} \mathcal{M}^2_{SS} &= \text{Re}(\mathcal{M}^2_{\phi\phi\dagger}) + \mathcal{M}^2_{\phi\phi} \,, \\ \mathcal{M}^2_{PP} &= \text{Re}(\mathcal{M}^2_{\phi\phi\dagger}) - \mathcal{M}^2_{\phi\phi} \,, \\ \mathcal{M}^2_{SP} &= -\text{Im}(\mathcal{M}^2_{\phi\phi\dagger}) \,, \end{aligned} \tag{15}$$

respectively. If $\text{Im}(\mathcal{M}^2_{\phi\phi\dagger})$ vanishes, the scalars and pseudo-scalars decouple from one another and the unphysical Goldstone mode would be found among the latter. Finally, we note that the B_α entries may also be considered as a kind of LR mixing.

We would like to emphasize that the above scalar mass results are complete — all RPV contributions, SUSY breaking or otherwise, are included. The simplicity of the result is

a consequence of the SVP. Explicitly, there are no RPV A-term contributions due to the vanishing of VEVs $v_i \equiv \sqrt{2}\langle \hat{L}_i \rangle$. The Higgs-boson-slepton results given as in Eqs.(9) and (14) contain a redundancy of parameters and hide the unphysical Goldstone state. However, the results as they are given here are good enough for some purposes including the present EDM discussion.

Note that in the following discussion, we will not consider flavor changing scalar mass terms from soft SUSY breaking, which could be suppressed through a flavor-blind SUSY breaking mediating mechanism such as gauge mediation. A major concentration of our study, however, will be on the effects of the flavor changing scalar mass terms from RPV superpotential parameters, which give interesting new results.

IV. CONTRIBUTIONS TO NEUTRON EDM AT 1-LOOP

In this section, we will discuss the RPV 1-loop contributions to neutron EDM systematically, drawing comparison with the R-parity conserving (MSSM) case wherever it would be useful. We will give complete 1-loop formulae for quark EDM's for our generic supersymmetric SM. We will not, however, go into the chromoelectric dipole operator or Weinberg gluonic operator contributions. Following the common practice, family mixing will largely be neglected, though we will comment on some particularly interesting aspects of the issue. We will also compare the results with Feynman diagrams given more or less in an electroweak basis. Naively, such diagrams, with a minimal number of mass insertions admitted, should represent a first order result, at least where mass mixings are small. Note that the latter is true for the small-μ_i scenario, which is our major focus. Afterall, a mass eigenstate result may be considered as corresponding to taking an infinite summation over electroweak-state diagrams with all possible mass insertions. The comparison helps to illustrate better the physics hidden behind the complicated formulae. In addition to a short Letter by the present authors [3], some parts of the results here have also been discussed in Ref. [4].

A. Gluino Contributions

The most direct contributions come from a gaugino loop, as shown in Fig. 1. The diagram looks the same as the MSSM gluino and neutralino diagrams with two gauge coupling vertices. As pointed out in our previous short Letter [3], the new RPV contributions here are a simple result of the RPV LR squark mixings [*cf.* Eq.(8)]. In Ref. [3], we focused on the dominant gluino loop contribution. We first give some more details of that analysis before going into the other contributions. Notice that though both the u and d quarks get EDMs from gaugino loops in the the MSSM, only the d quark has the RPV contribution. The u-squark sector simply has no RPV LR mixings. In Fig. 1, as well as the subsequent

diagrams, we use a family index k for the external quark lines though only the $k = 1$ case would be the d- (or u-) quark EDM we are mainly concerned with. With the only possible exception of d_2, which corresponds to the s quark [15], $k \neq 1$ results are not relevant for neutron EDM.

For illustrative purposes, we first neglect interfamily mixings among the squarks. The $\tilde{d}$ mass-squared matrix, of the form given in Eq.(6) but reduced to one family, is Hermitian and can be diagonalized by the unitary transformation

$$\mathcal{D}_d^\dagger \, \mathcal{M}_D^2 \, \mathcal{D}_d = \mathrm{diag}\{ M_{\tilde{d}-}^2, M_{\tilde{d}+}^2 \} \; , \tag{16}$$

with

$$M_{\tilde{d}\mp}^2 = \frac{1}{2} \; \left[(\mathcal{M}_{LL}^2 + \mathcal{M}_{RR}^2) \mp \sqrt{(\mathcal{M}_{LL}^2 - \mathcal{M}_{RR}^2)^2 + 4 \, |\mathcal{M}_{RL}|^2} \right] \tag{17}$$

and

$$\mathcal{D}_d = \begin{pmatrix} \cos\frac{\theta}{2} & -\sin\frac{\theta}{2} \, e^{-i\phi} \\ \sin\frac{\theta}{2} \, e^{-i\phi} & \cos\frac{\theta}{2} \end{pmatrix} \; . \tag{18}$$

Here, $\mathcal{M}_{RL}^2 = |\mathcal{M}_{RL}^2| \, e^{i\phi}$ and the range of θ can be choosen so that $-\frac{\pi}{2} \leq \theta \leq \frac{\pi}{2}$ with $\tan\theta = \frac{2\,|\mathcal{M}_{RL}^2|}{\mathcal{M}_{LL}^2 - \mathcal{M}_{RR}^2}$. In terms of the mass eigenstates $\tilde{d}_-$ and $\tilde{d}_+$, the gluino contribution to the EDM is then given by [16,20]

$$\left(\frac{d_d}{e} \right)_{\tilde{g}} = -\frac{2\alpha_s}{3\pi} \left[\mathrm{Im}(\Gamma_d^{11}) \, \frac{M_{\tilde{g}}}{M_{\tilde{d}-}^2} \, \mathcal{Q}_{\tilde{d}} \, B\!\left(\frac{M_{\tilde{g}}^2}{M_{\tilde{d}-}^2} \right) + \mathrm{Im}(\Gamma_d^{12}) \, \frac{M_{\tilde{g}}}{M_{\tilde{d}+}^2} \, \mathcal{Q}_{\tilde{d}} \, B\!\left(\frac{M_{\tilde{g}}^2}{M_{\tilde{d}+}^2} \right) \right] \; , \tag{19}$$

where $\mathcal{Q}_{\tilde{d}} = -\frac{1}{3}$, $\Gamma_d^{1k} = \mathcal{D}_{d2k} \mathcal{D}_{d1k}^*$, giving $\mathrm{Im}(\Gamma_d^{11}) = -\mathrm{Im}(\Gamma_d^{12}) = \frac{1}{2} \sin\theta \, \sin\phi$, and

$$B(x) = \frac{1}{2\,(x-1)^2} \left[1 + x + \frac{2\,x \ln x}{(1-x)} \right] \; . \tag{20}$$

Introducing $M_{\tilde{d}}^2 = (M_{\tilde{d}-}^2 + M_{\tilde{d}+}^2)/2$ and using the identity relation $x\,B(x) = B(1/x)$, the gluino contribution becomes the often-quoted

$$\left(\frac{d_d}{e} \right)_{\tilde{g}} = -\frac{2\alpha_s}{3\pi} \, \frac{M_{\tilde{g}}}{M_{\tilde{d}}^2} \, \mathcal{Q}_{\tilde{d}} \, \mathrm{Im}(\delta_{11}^D) \, F\!\left(\frac{M_{\tilde{g}}^2}{M_{\tilde{d}}^2} \right) \; , \tag{21}$$

where δ_{11}^D is $\mathcal{M}_{RL}^2/M_{\tilde{d}}^2$ (with $\mathcal{M}_{RL}^2$ restricted to the $\tilde{d}$ family) and

$$F(x) = \frac{1}{(1-x)^3} \left[\frac{1+5x}{2} + \frac{(2+x)x \ln x}{(1-x)} \right] \; . \tag{22}$$

The EDM expression above is, in fact, the same as that of the MSSM case, except that δ_{11}^D, or equivalently $\mathcal{M}_{RL}^2$, has now an extra RPV part. From the general result given in Eq.(8), we have, for the $\tilde{d}$ squark,

$$\delta^D_{11} M^2_{\tilde{d}} = [A_d - \mu_0^* \tan\beta]\; m_d \; + \frac{\sqrt{2}\, M_W \cos\beta}{g_2}\, \delta A^D_{11} - \frac{\sqrt{2}\, M_W \sin\beta}{g_2}\, (\, \mu_i^* \lambda'_{i11}\,) \; . \tag{23}$$

Note that the $\mu_i^* \lambda'_{i11}$ term does contain nontrivial CP violating phases and gives RPV contributions to neutron EDM. Though the above analysis neglects interfamily mixings, it is clear from Fig. 1 that the LR squark mixing δ^D_{11} is what is directly responsible for the EDM contribution. Including interfamily mixings would complicate the mass eigenstate analysis but not modify the EDM result in any substantial way.

B. Neutralinolike Contributions

The contributions from the (electroweak) neutral gaugino loop, as shown in Fig. 1, are expected to be small, due to the much smaller gauge couplings. Apart from the neutral gaugino loops, there may be other neutralinolike loop contributions. In the MSSM, one has to consider possible contributions from the Higgsino parts and the gaugino-Higgsino mixing parts. Part of such contributions involves no LR squark mixing. The latter feature compensates for the smaller Yukawa-type couplings involved [19]. Without R parity, the gauginos and Higgsinos mix with the leptons. We have seven neutral fermions, all among which give rise to a neutralinolike loop contribution.

The neutral fermion loop contribution to u and d quark EDMs is given by

$$\left(\frac{d_f}{e}\right)_{\chi^0} = \frac{\alpha_{\rm em}}{4\pi\, \sin^2\theta_W}\, \mathcal{Q}_{\tilde{f}} \sum_{\tilde{f}_\mp} \sum_{n=1}^{7} {\rm Im}(\mathcal{N}_{fn\mp})\, \frac{M_{\chi^0_n}}{M^2_{\tilde{f}\mp}}\, B\!\left(\frac{M^2_{\chi^0_n}}{M^2_{\tilde{f}\mp}}\right) \; , \tag{24}$$

where

$$\begin{aligned}
\mathcal{N}_{fn-} = & \left[-\sqrt{2}\,\{\tan\theta_W\,(\mathcal{Q}_f - T_{3f})\, \boldsymbol{X}_{1n} + T_{3f}\, \boldsymbol{X}_{2n}\}\, \mathcal{D}^*_{f11} - \frac{y_f}{g_2}\, \boldsymbol{X}_{bn}\, \mathcal{D}^*_{f21} \; - \delta_{b4}\, \frac{\lambda'_{k11}}{g_2}\, \boldsymbol{X}_{(k+4)n}\, \mathcal{D}^*_{d21}\right] \\
& \cdot \left[\sqrt{2}\, \tan\theta_W\, \mathcal{Q}_f\, \boldsymbol{X}_{1n}\, \mathcal{D}_{f21} - \frac{y_f}{g_2}\, \boldsymbol{X}_{bn}\, \mathcal{D}_{f11} \; - \delta_{b4}\, \frac{\lambda'_{h11}}{g_2}\, \boldsymbol{X}_{(h+4)n}\, \mathcal{D}_{d11}\right] \; , \\
\mathcal{N}_{fn+} = & \left[-\sqrt{2}\,\{\tan\theta_W\,(\mathcal{Q}_f - T_{3f})\, \boldsymbol{X}_{1n} + T_{3f}\, \boldsymbol{X}_{2n}\}\, \mathcal{D}^*_{f12} - \frac{y_f}{g_2}\, \boldsymbol{X}_{bn}\, \mathcal{D}^*_{f22} \; - \delta_{b4}\, \frac{\lambda'_{k11}}{g_2}\, \boldsymbol{X}_{(k+4)n}\, \mathcal{D}^*_{d22}\right] \\
& \cdot \left[\sqrt{2}\, \tan\theta_W\, \mathcal{Q}_f\, \boldsymbol{X}_{1n}\, \mathcal{D}_{f22} - \frac{y_f}{g_2}\, \boldsymbol{X}_{bn}\, \mathcal{D}_{f12} \; - \delta_{b4}\, \frac{\lambda'_{h11}}{g_2}\, \boldsymbol{X}_{(h+4)n}\, \mathcal{D}_{d12}\right] \; ,
\end{aligned} \tag{25}$$

with $b = 3\,(4)$ for $T_{3f} = \frac{1}{2}\,(-\frac{1}{2})$ [*i.e.,* for f being the u (d) quark], and y_f the corresponding Yukawa coupling [*cf.* Eq.(4)]. Recall, from Eq.(16), that $\tilde{d}_\mp$ denotes the two $\tilde{d}$ mass eigenstates and $\mathcal{D}_d$ the diagonalizing matrix; likewise, $\tilde{u}_\mp$ and $\mathcal{D}_u$ are the corresponding notations for the u-quark case. Finally, the $\boldsymbol{X}_{ij}$'s are elements of the matrix that diagonalizes $\mathcal{M}_{\mathcal{N}}$, as defined explicitly in the Appendix. Note that the last term in each set of brackets of the $\mathcal{N}_{fn\mp}$ expressions is nonvanishing only for $f = d$, as indicated by the δ_{b4} symbol. Similar

to the case of the gaugino contributions, RPV contributions here exist only for the d-quark EDM. We would like to emphasize that the formulae here represent the full 1-loop result for our generic supersymmetric SM.

Each expression for $\mathcal{N}_{fn\mp}$ above is a product of two terms, from the two loop vertices involving the L- and R-handed quark fields, respectively, as a chirality flip has to be imposed within the loop. For each vertex, the three terms (in each set of brackets) correspond to the gauge, quark Yukawa, and RPV λ' couplings, with the last existing only for the d-quark case. With two gauge coupling vertices, we have the gaugino diagram. Diagrams with a gauge and a y_f coupling are shown explicitly in Fig. 2 for the d quark, in which y_d is indicated by λ'_{0kk}, *i.e.,* with the notation used in our superpotential and a general, unspecified, quark family index ($y_d \equiv \lambda'_{011}$ in our notation). Note that the diagrams require no LR mixing on the squark line. This is the important MSSM contribution, the chargino counterpart of which typically receives the major attention. The latter is numerically a bit larger. The type of diagrams has no RPV contribution.

There is, however, a RPV analogue to Fig. 2. With the notation as given, this is obviously given by replacing λ'_{0kk} in the figure with a RPV λ'_{ikk}. This is shown explicitly in Fig. 3. From the latter figure, one can see the the first order result would come from a l^0_i-gaugino mass mixing. However, under our formulation, the latter is vanishing [see Eq.(A8) in the Appendix]. Looking at the type of contributions from our EDM formula here, while a λ'_{k11} coupling may not be small, it comes into the formula with a $\boldsymbol{X}_{(k+4)n}$. For n = 1–4, corresponding to the heavy neutralino mass eigenstates, $\boldsymbol{X}_{(k+4)n}$ measures a RPV mixing in the neutral fermion masses $\mathcal{M}_{\mathcal{N}}$. For n = 5–7, at least one of the three $\boldsymbol{X}_{(k+4)n}$'s is expected to be of order 1, but the corresponding (physical neutrino) mass eigenvalues $M_{\chi^0_n}$'s give a strong suppression factor in the resulting EDM contributions. There is also a further suppression from the mixing factor of the gaugino part, *e.g.,* $\boldsymbol{X}_{1(k+4)}$. Furthermore, there is, potentially, a GIM cancellation among the seven mass eigenstates. Our numerical results, however, do show that the type of contribution is generally important. We will discuss the issue more carefully below, using the explicit example of its charginolike counterpart.

Last, we come to the diagrams with no gauge vertices, which we show in Fig. 4 for the d quark, using our generic $\lambda'_{\alpha jk}$ notation. Such a diagram in the MSSM case is totally negligible due to the small Yukawa couplings involved and the suppression from the LR squark mixing required. In fact, as shown in the figure, the minimal mass insertion needed for the diagram corresponds to a Majorana mass among the l^0_α's, which is again vanishing. The situation is similar to that of Fig. 3. The contribution is expected to be always dominated by the latter one.

C. Charginolike Contributions

Next we come to the charged fermion counterpart. With similar notation as used in the neutral fermion loop formula above, the charged fermion loop contributions to u- and d-quark EDMs can be written as

$$\left(\frac{d_f}{e}\right)_{\chi^-} = \frac{\alpha_{\rm em}}{4\pi\,\sin^2\theta_W}\,\sum_{\tilde{f}'\mp}\sum_{n=1}^{5}\,{\rm Im}(\mathcal{C}_{fn\mp})\,\frac{M_{\chi_n^-}}{M^2_{\tilde{f}'\mp}}\,\left[\mathcal{Q}_{\tilde{f}'}\,B\!\left(\frac{M^2_{\chi_n^-}}{M^2_{\tilde{f}'\mp}}\right)+(\mathcal{Q}_f-\mathcal{Q}_{\tilde{f}'})\,A\!\left(\frac{M^2_{\chi_n^-}}{M^2_{\tilde{f}'\mp}}\right)\right]\,, \tag{26}$$

for f being u (d) quark and f' being d (u), where

$$\begin{aligned}
\mathcal{C}_{un-} &= \frac{y_u}{g_2}\,\boldsymbol{V}^*_{2n}\,\mathcal{D}_{d11}\,\left(-\boldsymbol{U}_{1n}\,\mathcal{D}^*_{d11}+\frac{y_d}{g_2}\,\boldsymbol{U}_{2n}\,\mathcal{D}^*_{d21}+\frac{\lambda'_{k11}}{g_2}\,\boldsymbol{U}_{(k+2)n}\,\mathcal{D}^*_{d21}\right)\,,\\
\mathcal{C}_{un+} &= \frac{y_u}{g_2}\,\boldsymbol{V}^*_{2n}\,\mathcal{D}_{d12}\,\left(-\boldsymbol{U}_{1n}\,\mathcal{D}^*_{d12}+\frac{y_d}{g_2}\,\boldsymbol{U}_{2n}\,\mathcal{D}^*_{d22}+\frac{\lambda'_{k11}}{g_2}\,\boldsymbol{U}_{(k+2)n}\,\mathcal{D}^*_{d22}\right)\,,\\
\mathcal{C}_{dn-} &= \left(\frac{y_d}{g_2}\,\boldsymbol{U}_{2n}+\frac{\lambda'_{k11}}{g_2}\,\boldsymbol{U}_{(k+2)n}\right)\mathcal{D}_{u11}\,\left(-\boldsymbol{V}^*_{1n}\,\mathcal{D}^*_{u11}+\frac{y_u}{g_2}\,\boldsymbol{V}^*_{2n}\,\mathcal{D}^*_{u21}\right)\,,\\
\mathcal{C}_{dn+} &= \left(\frac{y_d}{g_2}\,\boldsymbol{U}_{2n}+\frac{\lambda'_{k11}}{g_2}\,\boldsymbol{U}_{(k+2)n}\right)\mathcal{D}_{u12}\,\left(-\boldsymbol{V}^*_{1n}\,\mathcal{D}^*_{u12}+\frac{y_u}{g_2}\,\boldsymbol{V}^*_{2n}\,\mathcal{D}^*_{u22}\right)\,,
\end{aligned}$$

(only repeated index i is to be summed) ; (27)

$\boldsymbol{V}$ and $\boldsymbol{U}$ are diagonalizing matrices of the charged fermion mass matrix $\mathcal{M}_c$ as defined by Eq.(A2) in the Appendix; and the function $A(x)$ is given by

$$A(x) = \frac{1}{2\,(1-x)^2}\left(3-x+\frac{2\ln x}{1-x}\right)\,. \tag{28}$$

The first and second parts of Eq.(26) come from the cases in which the photon is emitted from the squark and fermion lines inside the loop, respectively.

The basic feature of the $\mathcal{C}_{fn\mp}$'s terms is similar to the previous case of $\mathcal{N}_{fn\mp}$. They do not give rise to a charged gaugino loop contribution, though, as R-handed quarks do not couple to $\tilde{W}^\pm$. Taking the available gauge coupling term within each $\mathcal{C}_{fn\mp}$ and a y_f to form an admissible product, we have the contribution corresponding to a diagram in Fig. 5. This is the dominating MSSM contribution, besides the equally competitive gluino one. Note again that no LR squark mixing is required the diagrams.

The diagram given in Fig. 5b has the RPV analogue, which requires a l_k^-–$\tilde{W}^+$ mass insertion for the first order result, as shown in in Fig. 6. This is the $SU(2)$ partner of Fig. 3, something we promise to discuss in more detail. Looking at the contributions from our EDM formula here, we have again a λ'_{k11} coming in with a $\boldsymbol{U}_{(k+2)n}$, as versus the $\boldsymbol{X}_{(k+4)n}$ in the neutral case above. For n = 1–2, corresponding to the heavy chargino mass eigenstates,

$\boldsymbol{U}_{(k+2)n}$ measures a RPV mass mixing; it is of order 1 for $n = k+2$, but then $M_{\chi_n^-}$ is the small m_k, roughly the charged lepton mass. When one sums over for $n = 1$–5, it is easy to see that the result is proportional to the imaginary part of

$$\sum_{n=1}^{5} \boldsymbol{V}^*_{1n}\, M_{\chi_n^-} \boldsymbol{U}_{(k+2)n}\, F_{BA}\Big(M^2_{\chi_n^-}\Big)\ \lambda'_{k11}\ , \tag{29}$$

where $F_{BA}\Big(M^2_{\chi_n^-}\Big)$ denotes a function on $M^2_{\chi_n^-}$ corresponding to the large brackets in Eq.(26) with functions B and A. If the F_{BA} could be factored out, together with λ'_{k11}, what is left inside the summation is nothing other than the l_k^-–$\tilde{W}^+$ mass term, which is zero. This is a GIM-like cancellation mechanism, violated only to the extent that the loop integrals involved as given by the B and A functions are not universal. Our numerical calculations, however, show that the cancellation is very substantially violated, for generic values of chargino masses. Let us then look at the contribution from an individual mass eigenstate more closely. To get an analytical approximation, we used the perturbative results for $\boldsymbol{U}_{(k+2)n}$ given in the Appendix. For the $n = 1$ and 2 parts in the above sum, we have

$$\boldsymbol{V}^*_{1a}\, \mu^*_k\, R_{R_{2a}} F_{BA}\Big(M^2_{ca}\Big)\ \lambda'_{k11}\ , \tag{30}$$

with basically the same source of RPV complex phase as the gluino case, namely, from $\mathrm{Im}(\mu^*_k \lambda'_{k11})$, except that it is one value of k for each diagram here. Note that the explicit M_{ca} factors are canceled. The $n = k+2$ part is largely suppressed due to a small mass eigenvalue and the very small RPV R-handed mixing given by $\boldsymbol{V}^*_{1(k+2)}$ as shown in the Appendix. Note that $\boldsymbol{V}^*_{1a} \simeq R^*_{R_{1a}}$, and R_R is a 2×2 unitary matrix of order 1 elements. The expressions give an idea about the strength of the RPV contributions. In the limit of degenerate charginos, *i.e.,* $M_{c1} = M_{c2}$, the F_{BA} function factors out of the sum of the $n = 1$ and 2 parts and the GIM-like cancellation is clearly illustrated, simply from the unitarity of R_R. In fact, our numerical calculations give a cancellation up to 1 part in 10^4 in such a situation if we enforce the condition. However, that requires a every substantial complex phase for μ_0, hence of not the most phenomenological interest. Another interesting point on the parameter space appears when the R_R matrix is diagonal, at which the contribution also goes away, as is obvious from the above expression. This happens at the point where the condition $M_2^* \sin\beta = \mu_0 \cos\beta$ is satisfied. This feature will be confirmed by our numerical results presented below.

The rest of the charginolike contributions each has at least one y_f coupling and no gauge coupling vertex. Again, a LR squark mixing is required. However, of the first order electroweak-state diagrams, as depicted in Fig. 7, each has an admissible μ^*_α mass insertion on the fermion line. This looks a bit different from the neutral case above. Apart from an admissible RPV down-squark mixing for the case of the u quark, a RPV diagram again has the RPV parameter combination $\mu^*_k \lambda'_{k11}$ (no sum). Except for large-μ_i case, there is no

reason to expect the contribution to be of any significance compared to the other major contributions.

Our EDM formulae neglect interfamily mixings. However, general, unspecified, family indices are use in our figures to make the flavor structure transparent. We note that in the case of the contributions depicted by Figs. 4 and 7, off-diagonal $\mu_i^* \lambda'_{ijk}$-type RPV mixings could play a role to let the higher family squarks mediating more important contributions to u- and d-quark EDMs.

D. The Quark-Scalar Loop Contributions in Brief

There are superpartners to the diagrams in Fig. 7, *i.e.,* with quarks and charged scalars running inside the loop and a B_α coupling on the scalar line. These diagrams are shown explicitly in Fig. 8. Here, the $\alpha = 0$ case gives the MSSM charged Higgs boson contribution. With the B_i's, we have the RPV contributions. Analytically, we have the formula

$$\left(\frac{d_f}{e}\right)_{\phi^-} = \frac{\alpha_{\rm em}}{4\pi\,\sin^2\theta_W} \sum_m{}' \sum_{n=1}^{3} {\rm Im}(\mathcal{C}^{L}_{inm}\,\mathcal{C}^{R^*}_{inm})_f\,\frac{M_{f'_n}}{M^2_{\tilde{\ell}_m}}\,\left[(\mathcal{Q}_f - \mathcal{Q}_{f'})\,B\!\left(\frac{M^2_{f'_n}}{M^2_{\tilde{\ell}_m}}\right) + \mathcal{Q}_{f'}\,A\!\left(\frac{M^2_{f'_n}}{M^2_{\tilde{\ell}_m}}\right)\right]\,, \tag{31}$$

where, for $f = u$,

$$\begin{aligned}
\mathcal{C}^{R}_{inm} &= \frac{y_d}{g_2}\,\mathcal{D}^{l^*}_{1m} + \frac{\lambda'^*_{i1k}}{g_2}\,\mathcal{D}^{l^*}_{(i+2)m}\,,\\
\mathcal{C}^{L}_{inm} &= \frac{y_u}{g_2}\,\mathcal{D}^{l^*}_{2m}\,,
\end{aligned} \tag{32}$$

and, for $f = d$,

$$\begin{aligned}
\mathcal{C}^{R}_{inm} &= \frac{y_u}{g_2}\,\mathcal{D}^{l}_{1m}\,,\\
\mathcal{C}^{L}_{inm} &= \frac{y_d}{g_2}\,\mathcal{D}^{l}_{2m} + \frac{\lambda'_{ij_1}}{g_2}\,\mathcal{D}^{l}_{(i+2)m}\,,
\end{aligned} \tag{33}$$

with the $\sum'_m$ denoting a sum over (seven) nonzero mass eigenstates of the charged scalar; *i.e.,* the unphysical Goldstone mode is dropped from the sum, $\mathcal{D}^l$ being the diagonalization matrix, *i.e.,* $\mathcal{D}^{l\dagger}\mathcal{M}^2_E\,\mathcal{D}^l = {\rm diag}\{\,M^2_{\tilde{\ell}_m}, m = 1\!-\!8\,\}$.

With similar notation as used in the charged scalar loop formula above, the neutral scalar loop contributions to the EDMs can be written as

$$\left(\frac{d_f}{e}\right)_{\phi^0} = \frac{\alpha_{\rm em}}{4\pi\,\sin^2\theta_W} \sum_m{}' \sum_{n=1}^{3} {\rm Im}(\mathcal{N}^{L}_{inm}\,\mathcal{N}^{R^*}_{inm})\,\frac{M_{f_n}}{M^2_{S_m}}\,\mathcal{Q}_f\,A\!\left(\frac{M^2_{f_n}}{M^2_{S_m}}\right)\,, \tag{34}$$

where, for $f = u$,

$$\mathcal{N}^{R}_{inm} = -\frac{y_u}{g_2}\,\frac{1}{\sqrt{2}}\,[\mathcal{D}^{s}_{1m} - i\,\mathcal{D}^{s}_{6m}]\;,$$
$$\mathcal{N}^{L}_{inm} = -\frac{y_u}{g_2}\,\frac{1}{\sqrt{2}}\,[\mathcal{D}^{s}_{1m} + i\,\mathcal{D}^{s}_{6m}]\;, \tag{35}$$

and, for $f = d$,

$$\mathcal{N}^{R}_{inm} = -\frac{y_d}{g_2}\,\frac{1}{\sqrt{2}}\,[\mathcal{D}^{s}_{2m} - i\,\mathcal{D}^{s}_{7m}] - \frac{\lambda'^{*}_{h1k}}{g_2}\,\frac{1}{\sqrt{2}}\,[\mathcal{D}^{s}_{(h+2)m} - i\,\mathcal{D}^{s}_{(h+7)m}]\;,$$
$$\mathcal{N}^{L}_{inm} = -\frac{y_d}{g_2}\,\frac{1}{\sqrt{2}}\,[\mathcal{D}^{s}_{(i+2)m} + i\,\mathcal{D}^{s}_{(i+7)m}] - \frac{\lambda'_{hk1}}{g_2}\,\frac{1}{\sqrt{2}}\,[\mathcal{D}^{s}_{(h+2)m} + i\,\mathcal{D}^{s}_{(h+7)m}]\;, \tag{36}$$

with again the unphysical Goldstone mode to be dropped from the sum over scalar mass eigenstates (nine nonzero), and the obvious notation $(\mathcal{D}^{s})^{T}\,\mathcal{M}^{2}_{S}\,\mathcal{D}^{s} = \mathrm{diag}\{\, M^{2}_{S_m}, m = 1-10\,\}$, $\mathcal{D}^{s}$ being an orthogonal matrix.

Note that the formulae given in this section, like those in the rest of the paper, have neglected CKM mixings among the quarks. However, unlike the previous cases, the mixings play an important role in the quark-scalar loop contributions. This is a result of the fact that the EDM contributions have a fermion, a quark in this case, mass dependence, and the mass hierarchy among the quarks. For instance, the top quark loop is expected to give a dominating contribution. Generalizing the formulae to include the mixings is straightforward. The formulae as they are given in this subsection do give a basic illustration of the major analytical structure of the type of contributions. We will only discuss the features briefly here.

Diagrams depicting the neutral scalar contributions are like superpartners of the type of diagram given in Fig. 3. This is shown in Fig. 8 for both the u- and d-quark cases. Such a diagram could be interpreted as requiring a Majorana-like scalar mass insertion. The latter is first considered in Ref. [11], under the name of Majorana masses from the "sneutrinos". However, looking at it from the present framework, these diagrams should be interpreted as having Majorana-like mass insertions among the l^{0}_{α}'s (and h^{0}_{u} for the case of the u quark).

The quark-scalar loops given by the above formulae are not quite considered in the case of the MSSM, as they would be suppressed by the very small Yukawa couplings. The RPV analogue, however, admits much more general flavor structure, as illustrated in the diagrams in Figs. 8 and 9. For instance, a top quark with order-1 Yukawa coupling could be contributing to the d-quark EDM through a charged scalar loop. Contributions discussed in this subsection depend on a much larger number of parameters, through the scalar mass matrices [*cf.* Eqs.(9)–(15)]. The extra parameters are related directly to Higgs physics. The important RPV B_i parameters here have a strong connection with the μ_i's [23]. Furthermore, the more general flavor structure involved means that the EDM contributions involve λ'_{ijk} couplings that would also have important roles to play in the related processes of $b \to s\,\gamma$ and $b \to d\,\gamma$. We will leave all these issues for later studies.

V. RESULT FROM NUMERICAL CALCULATIONS

We now discuss the results we obtained by a careful numerical implementation of our EDM formulae discussed above, with explicit numerical diagonalization of all the mass matrices involved. Note that the quark-scalar loop contribution is not included in the numerical study. Hence, we are concentrating on the SUSY contributions in the presence of RPV couplings, to be compared directly with the MSSM results.

As discussed in the previous section, the imaginary part of the combination $\mu_i^* \lambda'_{i11}$ is what is central to the RPV 1-loop EDM contributions. To simplify the discussion, we single out μ_3 and λ'_{311} and put the corresponding parameters for $i = 1$ and 2 to be essentially zero [3]. This applies to all the numerical results discussed here.

We give in Table 1 some detailed numerical results for four illustrative sample cases. To first focus on the RPV contributions which we are particularly interested in, cases A and B in the table have all complex phases in the R-parity conserving part switched off. For the RPV parameters μ_3 and λ'_{311}, we take the former being real and put a $\pi/4$ complex phase into the latter. However, we want to emphasize again that only the phase of the combination $\mu_3^* \lambda'_{311}$ matters. For instance, we have checked explicitly that shifting the overall phase, or a part of it into μ_3 instead, gives exactly the same results. The difference bewteen case A and case B is only in the value of μ_3 chosen. Case A has small μ_3, at $10^{-3}\,\mathrm{GeV}$. This is the small-μ_i scenario, corresponding to a sub-eV mass for ν_τ as suggested, but far from mandated, by the result from the Super-Kamiokande (super-K) experiment [24] [4]. In contrast, case B has $\mu_3 = 1\,\mathrm{GeV}$. Note that imposing the 18.2 MeV experimental bound [25] for the mass of ν_τ still admits a relatively large μ_3, especially for a large $\tan\beta$. Reading from the results in Ref. [7], the bound is $\sim 7\,\mathrm{GeV}$ at $\tan\beta = 2$ and $\sim 300\,\mathrm{GeV}$ at $\tan\beta = 45$. As for λ'_{311}, the best bound on the (from $\tau \to \pi\nu$) is around 0.05–0.1 [26]. Hence, case B is still within the admissible region of RPV parameter space, though beyond the more popular small-μ_i scenario. Moreover, we have illustrated in Ref. [3] that the λ'_{311} bound is not strengthened even when the above-mentioned stringently interpreted neutrino mass bound from super-K is imposed on the 1-loop neutrino mass contribution obtainable from the parameter. We therefore use the same λ'_{311} magnitude of 0.05 for both, and actually all, cases in the table.

Apart from the overall EDM results, we are interested in understanding the relative

---

[3] In the actual calculation, tiny but nonzero values are used to avoid possible problems of numerical manipulations.

[4] Note that $\mu_3 \cos\beta \sim 10^{-4}\,\mathrm{GeV}$ is actually expected, allowing a larger μ_3 in the case of large $\tan\beta$ (see, for example, Ref. [8]). Our choice of μ_3 value here is, admittedly, quite pushing the limit. It is mainly for illustrative purposes.

values of the different pieces of the contributions discussed in the previous section. Hence, we show, in the table, the contribution from individual pieces, identified by the couplings of the two loop-vertices given inside the first column. They can be matched easily with terms in the formulae. The corresponding Feynman diagrams are marked whenever they are available inside the next column. Column 3 of the table indicates whether a LR squark mixing is involved in the contribution, and if the RPV part of the latter is available and needed for a RPV contribution to come in. The individual contribution that is vanishing under cases A and B corresponds to a diagram which does not admit a RPV contribution. This is the case for most entries for the u-quark EDM and the entries for the charginolike loop contributions to the d-quark EDM not involving a λ' coupling loop vertex. Note that a charginolike loop for the d quark involves LR mixing of $\tilde{u}$ which has no RPV part. As emphasized in Ref. [3], the RPV contributions are far more prominent for the d quark part. Again, λ'_{3ii} is the only nonzero λ' coupling introduced, though we use a more general λ' notation within the table to remind the readers of the more general flavor structure admissible, as illustrated in the previous section. We also recall from the discussions there that a λ'_{ijk} coupling always comes into the EDM picture accompanied by a RPV fermion mixing matrix element proportional to μ_i^*. The EDM results are basically in direct proportion to $\mu_i^*\,\lambda'_{i11}$ over the whole region of parameter space studied. Hence, comparing cases A and B, we see an *exact* factor of 10^{-3} suppression in case A for contributions with one λ' loop vertex or involving a RPV LR mixing, except the very small y_d^2 term.

The overall EDM numbers of case A are still below the present experimental bound. This is smaller than a naive estimated result, as given for the gluino contribution by Eq.(21), for example, due to some unavoidable partial cancellation. For the gluino result, in particular, the cancellation is between the contributions from the two squark mass eigenstates, which would in fact be exact when the latter states are degenerate. This slightly weakens the EDM bound of the previously estimated $\mathrm{Im}(\mu_i^*\lambda'_{i11}) < 10^{-6}\,\mathrm{GeV}$ result given in Ref. [3]. However, we see here that with a unification-type relationship imposed on the gaugino masses, we are likely to have a chargino contribution larger than the gluino one. Moreover, the values of the other SUSY parameters chosen here can be pushed to increase the EDM number, as discussed below. As for case B, the numbers are beyond the experimental bound, indicating that the RPV parameters, or the involved complex phase, would have to be further constrained.

Case C of Table 1 gives a different scenario. Here, we allow complex phases, and hence EDM contributions, of the MSSM part. The RPV parameters are set real. This ensures no RPV EDM contribution from diagrams involving LR squark mixings. The interesting point to note here is that there is indeed nonzero RPV contributions from diagrams with RPV loop vertices. In particular, the RPV chargino contribution to d-quark EDM is comparable in magnitude to its R-parity conserving counterpart. Hence, the existence of nonzero RPV parameters, even real, would change the EDM story of the MSSM. In other words, in the

presence of a complex μ_0, the neutron EDM bound actually constrains the magnitude of the the combination of RPV parameters given by $\mu_i^* \lambda'_{i11}$, instead of just the phase of it. This is an important feature that has not been pointed out before. The result of the case serves, otherwise, as a check against other neutron EDM studies of the MSSM.

Finally, we illustrate in case D a specific situation with both R-parity conserving and violating phases. Here, we pick a case of large $\tan\beta$, for which the larger μ_3 is still within the limit admitted by the stringent interpretation of the super-K bound [8]. The negative phase chosen for λ'_{311} gives a cancellation between the two contributions to the imaginary part of LR d squark mixing. This directly resulted in suppression of the EDM contributions involving the latter, such as the d-quark gluino loop. The very interesting point to note here is that the same cancellation results in the chargino and neutralino loop [5] , as explicitly illustrated by the entries of the terms with loop vertex couplings given by $g \cdot y_d$ and $g \cdot \lambda'_{i11}$ in both cases. Essentially, when we have a small imaginary part for $\mu_\alpha^* \lambda'_{\alpha 11}$ (recall that $\alpha = 0$ to 3, $\lambda'_{011} \equiv y_d$), *e.g.,* an internal cancellation among the summed terms, the corresponding d quark EDM contributions, involving the suppressed LR mixing [*cf.* first line of Eq.(8)] or otherwise, are all suppressed. The chargino and neutralino contributions actually reflect some proportionality to the (F-term) LR mixings in a way similar to the gluino contribution. Note, however, that the A-term phase contributes to the gluino diagram while leaving the charginolike and neutralinolike diagrams not quite affected, and hence spoils the simultaneous cancellation achieved in the case D results here. Besides, as the u-quark EDM results do not have a complete matching analogue between the R-parity conserving and violating contributions, the simultaneous cancellation mechanism does not exist there. In the current case, the u-quark parts are suppressed due to large $\tan\beta$.

The above sample cases illustrate some of the interesting features about the RPV contributions to neutron EDM. Next, we discuss how the EDM result varies with some basic parameters. Fig. 10 shows a logarithmic plot of (the magnitude of) the RPV neutron EDM result for μ_0 value between $\pm 2000\,\mathrm{GeV}$, with the other parameters set at the same values as case A in Table 1. Note the the small $|\mu_0|$ ($\lesssim 70\,\mathrm{GeV}$) region has been ruled out for having too light a chargino mass [7]. As noted in the previous section, the gluino and chargino contributions compete with one another with one of them being dominating in a region of the parameter space. The dip on the C line for the charginolike contribution corresponds

---

[5] A chargino (neutralino) contribution means exactly the one with a physical chargino (neutralino) running in the loop. Hence, it is only a part of the fermion mass eigenstate sum in the analytical formulae given for the (total) charginolike and neutralinolike loop contributions. The latter, as illustrated in the previus section, are generally dominated by the chargino and neutralino mass eigenstates.

to the case of vanishing R-handed mixing among the charginos, *i.e.,* when the condition $M_2 \sin\beta + \mu_0 \cos\beta = 0$ is satisfied, as noted above, where the contribution essentially vanishes. Note that in the region to the left of the point, the contribution becomes negative. The G line is horizontal, as the gluino diagram result has no dependence on μ_0.

Next, we check the tanβ dependence and compare with the MSSM result. In Fig. 11, we give again a plot of the (total) EDM result for the same set of input parameters as in case A of Table 1, while varying tanβ. This is the line marked as "RPV only". The numerical result confirms our earlier discussion that there is not much sensitivity in tanβ [*cf.* expression (30)], as indicated by the flatness of the line. This is in good contrast to the MSSM result, also based on the same set of input parameters except with nonvanishing phases for A and μ_0. The third line, marked by "GSSM", gives the total result obtained from our formulae given above with the same nonvanishing phases for A and μ_0, as well as λ'_{311}. Note that the GSSM result here is more than the sum of the two other lines, due to the presence of RPV contribution even in the limit of a real λ'_{311}, as discussed for Case C of Table 1 above. The tanβ dependence, or the lack of, illustrated in the figure is quite generic, in a wide region of the parameter space.

The dip in the GSSM line of Fig. 11 represents a point where the overall contribution is small as a result of the cancellation among the different pieces, a feature that has attracted a lot of attention lately in the case of the MSSM (see, for example, Ref. [27] and Refs. [20,21]). The MSSM line in the figure has a dip only beyond the range of the tanβ value shown. As also pointed out in a little bit different setting (with vanishing A phase) for Case D of Table 1 above, the new RPV contribution modifies the overall picture and provides a possible new cancellation mechanism. The cancellation feature is better illustrated in Fig. 12, in which the variation against the A-term phase is shown, for the small and large tanβ cases. Again our GSSM result is compared with that of the MSSM. One can see that the presence of the RPV contribution shifts the cancellation points substantially. Finally, we show variations of the result as a function of the gaugino mass parameters here represented by M_2. This is given in Fig. 13 with the four lines marked and correspond to the four cases of Fig. 12, each with the A-term phase set at the position of the dip as given in the latter figure.

VI. CONCLUSION

We have given explicit formulae and detailed discussions on the full 1-loop contributions to quark EDMs for the generic supersymmetric SM (without R parity). The extra, RPV, contributions are interesting additions to the R-parity conserving part. We have given results from an exact numerical study, illustrating various novel aspects. Our formulation emphasizes the universal structure of the R-parity conserving and violating parts, which also is illustrated itself well in the results. The experimental bound on the neutron EDM is hence

established as an important source of constraints on the model parameter space, including the RPV part. The 1-loop RPV contributions always involve the particular combination of RPV parameters given by $\mu_i^* \lambda'_{i11}$, with little sensitivity to the value of $\tan\beta$. So far as the RPV parameters are concerned, this combination is well constrained by the EDM bound. This applies not only to the complex phase, or imaginary part of, the combination. Real $\mu_i^* \lambda'_{i11}$ contribute in the presence of complex phases in the chargino and neutralino mass entries. Studies with either μ_i- or λ'- type couplings assumed to be zero miss the class of very interesting phenomenological features of SUSY without R parity.

ACKNOWLEDGMENTS

O.K. is in great debt to Kingman Cheung, a collaborator on a parallel work on $\mu \to e\,\gamma$, for discussions on common issues of the two studies. Y.Y.K. wishes to thank M. Kobayashi and H.Y. Cheng for their hospitality. His work was in part supported by the National Science Council of R.O.C. under Grant No. NSC-89-2811-M-001-0053.

APPENDIX A: NOTES ON THE FERMION MASSES

Under the SVP, the (color-singlet) charged fermion mass matrix is given by the simple form

$$\mathcal{M}_{\mathcal{C}} = \begin{pmatrix} M_{\scriptscriptstyle 2} & \sqrt{2}\, M_{\scriptscriptstyle W} \cos\beta & 0 & 0 & 0 \\ \sqrt{2}\, M_{\scriptscriptstyle W} \sin\beta & \mu_0 & \mu_1 & \mu_2 & \mu_3 \\ 0 & 0 & m_1 & 0 & 0 \\ 0 & 0 & 0 & m_2 & 0 \\ 0 & 0 & 0 & 0 & m_3 \end{pmatrix} , \tag{A1}$$

with explicit bases for right-handed and left-handed states given by $(-i\tilde{W}^+, \tilde{h}_u^+, l_1^+, l_2^+, l_3^+)$ and $(-i\tilde{W}^-, l_0^-, l_1^-, l_2^-, l_3^-)$, respectively. Here, we allow $M_{\scriptscriptstyle 2}$ and all four μ_α parameters to be complex, though the m_i's are restricted to be real, for reasons that will become clear below. Obviously, each μ_i parameter here characterizes directly the deviation of the l_i^- from the corresponding physical charged lepton ($\ell_i = e$, μ, and τ), *i.e.,* light mass eigenstates. For any set of other parameter inputs, the m_i's can then be determined, through a simple numerical procedure, to guarantee that the correct mass eigenvalues of m_e, m_μ, and m_τ are obtained — an issue first addressed and solved in Ref. [7]. The latter issue is especially important when μ_i's not substantially smaller than μ_0 are considered. Such an odd scenario is not definitely ruled out [7]. However, for the more popular small-μ_i scenario, we have $l_i^- \approx \ell_i^-$, and deviations on m_i's from the (real) ℓ_i masses are negligible. Note that the deviation of l_i^+ from ℓ_i^+ is quite negligible in any case.

We introduce unitary matrices $\boldsymbol{V}$ and $\boldsymbol{U}$ diagonalizing the R- and L-handed states with

$$\boldsymbol{V}^\dagger \mathcal{M}_{\mathcal{C}}\, \boldsymbol{U} = \mathrm{diag}\{M_{\chi_n^-}\} \equiv \mathrm{diag}\{M_{c1}, M_{c2}, m_e, m_\mu, m_\tau\} \; . \tag{A2}$$

Here, the mass eigenvalues $M_{\chi_n^-}$ with $n = 1$ and 2, *i.e.,* M_{c1} and M_{c2}, are the chargino masses. Consider further

$$R_{\scriptscriptstyle R}^\dagger \begin{pmatrix} M_{\scriptscriptstyle 2} & \sqrt{2}\, M_{\scriptscriptstyle W} \cos\beta \\ \sqrt{2}\, M_{\scriptscriptstyle W} \sin\beta & \mu_0 \end{pmatrix} R_{\scriptscriptstyle L} \;=\; \mathrm{diag}\{M_{c1}^o, M_{c2}^o\} \tag{A3}$$

with M_{c1}^o and M_{c2}^o being the chargino masses in the $\mu_i = 0$ limit. One can then write the diagonalizing matrices in the block form

$$\boldsymbol{V} = \begin{pmatrix} R_{\scriptscriptstyle R} & -R_{\scriptscriptstyle R}\, V^\dagger \\ V & I_{3\times 3} \end{pmatrix} \qquad\qquad \boldsymbol{U} = \begin{pmatrix} R_{\scriptscriptstyle L} & -R_{\scriptscriptstyle L}\, U^\dagger \\ U & I_{3\times 3} \end{pmatrix} \; . \tag{A4}$$

For $\mu_i \ll M_{ca}^o$ ($a = 1$ and 2), a block perturbative diagonalization can be performed directly on the matrix $\mathcal{M}_{\mathcal{C}}$ to obtain the following simple result

$$
\begin{aligned}
\boldsymbol{U}_{(i+2)1} &\simeq \frac{\mu_i^*}{M_{c1}}\, R_{_{R21}} \ , \\
\boldsymbol{U}_{(i+2)2} &\simeq \frac{\mu_i^*}{M_{c2}}\, R_{_{R22}} \ , \\
\boldsymbol{V}_{(i+2)a} &\simeq \frac{m_i}{M_{c_a}}\, \boldsymbol{U}_{(i+2)a} \qquad\qquad (a = 1 \,\text{and}\, 2) \ .
\end{aligned} \tag{A5}
$$

Elements in the $R_{_R}$ and $R_{_L}$ matrices are all expected to be of order 1. The above expressions illustrate the magnitudes of given matrix elements involving RPV mixings, as well as their dependence on the RPV parameters. We note that the L-handed mixings are roughly measured by the ratio of a μ_i to the chargino mass scale, while R-handed mixings are further suppressed by a charged lepton to chargino mass ratio, hence quite negligible under most consideration.

Note that the notation here is different from that given in Ref. [7] and many others in the literature. More explicitly, we have R- and L-handed mass eigenstates given by $(\,\chi_{+n}\,) = \boldsymbol{V}^T\,[-i\tilde{W}^+, \tilde{h}_u^+, l_1^+, l_2^+, l_3^+\,]^T$ and $(\,\chi_{\text{-}n}\,) = \boldsymbol{U}^\dagger\,[-i\tilde{W}^{\text{-}}, l_0^{\text{-}}, l_1^{\text{-}}, l_2^{\text{-}}, l_3^{\text{-}}\,]^T$, which form the five Dirac fermions

$$
\chi_n^{\text{-}} = \begin{pmatrix} \chi_{\text{-}n} \\ \chi_{+n}^\dagger \end{pmatrix} \ .
$$

The $\boldsymbol{U}_{(i+2)a}$ elements as given above show no obvious dependence on $\tan\!\beta$, though some nontrivial dependence is expected through the $R_{_{R2a}}$ elements. Our exact numerical result also indicates a weak sensitivity on the $\tan\!\beta$ value here. On the other hand, we have, from Eqs.(A4) and (A5),

$$
\begin{aligned}
\boldsymbol{U}_{a(i+2)} &= -\mu_i \cdot \Big[R_{_L}\ (\mathrm{diag}\{M_{c1}^o, M_{c2}^o\})^{-1}\ R_{_R}^\dagger \Big]_{a2} \ , \\
\boldsymbol{V}_{a(i+2)} &= -\mu_i \cdot \Big[R_{_R}\ (\mathrm{diag}\{M_{c1}^o, M_{c2}^o\})^{-2}\ R_{_R}^\dagger \Big]_{a2} \ ,
\end{aligned} \tag{A6}
$$

giving the result

$$
\begin{aligned}
\boldsymbol{U}_{1(i+2)} &= \frac{\mu_i\, \sqrt{2}\, M_{_W} \cos\!\beta}{M_0^2} \ , \\
\boldsymbol{U}_{2(i+2)} &= -\frac{\mu_i\, M_2}{M_0^2} \ , \\
\boldsymbol{V}_{1(i+2)} &= \mu_i\, m_i\ \frac{\sqrt{2}\ M_{_W}(M_2^*\, \sin\!\beta + \mu_0\, \cos\!\beta)}{|M_0|^4} \ , \\
\boldsymbol{V}_{2(i+2)} &= -\mu_i\, m_i\ \frac{(|M_2|^2 + 2\, M_{_W}^2 \cos^2\!\beta)}{|M_0|^4} \ ,
\end{aligned} \tag{A7}
$$

where

$$
M_0^2 \ \equiv\ \mu_0\, M_2 - M_{_W}^2\, \sin\!2\beta = M_{c1}^o\, M_{c2}^o \ .
$$

These RPV elements correspond to those given in Ref. [7] (with all complex phases neglected), where the crucial $\cos\beta$ dependence of the nonstandard Z^0-boson couplings of the physical charged leptons ($\ell_i \equiv \chi_{i+2}$) through $\boldsymbol{U}_{1(i+2)}$ is emphasized. The difference between $\boldsymbol{U}_{(i+2)a}$ and $\boldsymbol{U}_{a(i+2)}$ is hence very important.

The 7×7 Majorana mass matrix for the neutral fermion can be written as

$$\mathcal{M}_{\mathcal{N}} = \begin{pmatrix} M_1 & 0 & M_Z \sin\theta_W \sin\beta & -M_Z \sin\theta_W \cos\beta & 0 & 0 & 0 \\ 0 & M_2 & -M_Z \cos\theta_W \sin\beta & M_Z \cos\theta_W \cos\beta & 0 & 0 & 0 \\ M_Z \sin\theta_W \sin\beta & -M_Z \cos\theta_W \sin\beta & 0 & -\mu_0 & -\mu_1 & -\mu_2 & -\mu_3 \\ -M_Z \sin\theta_W \cos\beta & M_Z \cos\theta_W \cos\beta & -\mu_0 & 0 & 0 & 0 & 0 \\ 0 & 0 & -\mu_1 & 0 & 0 & 0 & 0 \\ 0 & 0 & -\mu_2 & 0 & 0 & 0 & 0 \\ 0 & 0 & -\mu_3 & 0 & 0 & 0 & 0 \end{pmatrix} , \tag{A8}$$

with explicit basis $(-i\tilde{B}, -i\tilde{W}, \tilde{h}_u^0, \tilde{h}_d^0, l_1^0, l_2^0, l_3^0)$. Note that $\tilde{h}_d^0 \equiv l_0^0$, and, from the above discussion of the charged fermions, we have, for small μ_i's, $(l_1^0, l_2^0, l_3^0) \approx (\nu_e, \nu_\mu, \nu_\tau)$. The symmetric, but generally non-Hermitian, matrix can be diagonalized by using unitary matrix $\boldsymbol{X}$ such that

$$\boldsymbol{X}^T \mathcal{M}_{\mathcal{N}} \boldsymbol{X} = \mathrm{diag}\{M_{\chi_n^0}\} \; . \tag{A9}$$

Again, the first part of the mass eigenvalues, $M_{\chi_n^0}$ for $n = 1$–4 here, gives the heavy states, *i.e.,* neutralinos. The last part, $M_{\chi_n^0}$ for $n = 5$–7 are hence physical neutrino masses at the tree level.

REFERENCES

[1] For a recent review, see Y. Nir, hep-ph/9911321.

[2] R.M. Godbole, S. Pakvasa, S.D. Rindani, and X. Tata, Phys. Rev. **D61**, *113003* (2000); S.A. Abel, A. Dedes, and H.K. Dreiner, JHEP **05**, 013 (2000); see also D. Chang, W.-F. Chang, M. Frank, and W.-Y. Keung, Phys. Rev. **D62**, *095002* (2000) .

[3] Y.-Y. Keum and O.C.W. Kong, Phys. Rev. Lett. **86**, 393 (2001).

[4] K. Choi, E.J. Chun, and K. Hwang, Phys. Rev. **D63**, *013002* (2000).

[5] O.C.W. Kong, JHEP **0009**, 037 (2000).

[6] For more discussion on the formulation aspect, see O.C.W. Kong, IPAS-HEP-k008, *manuscript in preparation*.

[7] M. Bisset, O.C.W. Kong, C. Macesanu, and L.H. Orr, Phys. Lett. **B430**, 274 (1998); Phys. Rev. **D62**, *035001* (2000).

[8] O.C.W. Kong, Mod. Phys. Lett. **A14**, 903 (1999); Phys. At. Nucl. **63**, 1083 (2000).

[9] K. Cheung and O.C.W. Kong, Phys. Rev. **D61**, *113012* (2000).

[10] A. Abada and M. Losada, Nucl. Phys. **B585**, 45 (2000).

[11] Y. Grossman and H.E. Haber, hep-ph/9906310; see also S. Davidson and M. Losada, JHEP **0005**, *021* (2000).

[12] K. Cheung and O.C.W. Kong, IPAS-HEP-k007, hep-ph/0101347, *submitted to* Phys. Rev. **D**.

[13] K. Choi, E.J. Chun, and K. Hwang, Phys. Lett. **B488**, 145 (2000).

[14] O.C.W. Kong *et al.*, *work in progress*.

[15] See, for a review, X.-G. He, B.H.J. McKellar, and S. Pakvasa, Int. J. Mod. Phys. **A4**, 5011 (1989).

[16] T. Ibrahim and P. Nath, Phys. Rev. **D57**, 478 (1998); *Erratum — ibid* **D58**, *019901* (1998); *Erratum — ibid* **D60**, *079903* (1999); *Erratum — ibid* **D60**, *119901* (1999).

[17] R. Arnowitt, J.L. Lopez, and D.V. Nanopoilos, Phys. Rev. **D42**, 2423 (1990).

[18] P.G. Harris *et al.*, Phys. Rev. Lett. **82** 904 (1999).

[19] Y. Kizukuri and N. Oshimo, Phys. Rev. **D46**, 3025 (1992).

[20] T. Ibrahim and P. Nath, Phys. Rev. **D58**, *111301* (1998); *Erratum — ibid* **D60**, *099902* (1999).

[21] T. Goto, Y.-Y. Keum, T. Nihei, Y. Okada, and Y. Shimizu, Phys. Lett. **460B**, 333 (1999).

[22] L.E. Ibáñez and G.G. Ross, Nucl. Phys. **B368**, 3 (1992).

[23] See the appendix of Ref. [5].

[24] Super-Kamiokande Collaboration, Y. Fukuda *et al.*, Phys. Rev. Lett. **81**, 1562 (1998); P. Lipari, hep-ph/9904443; G.L. Fogli, E. Lisi, A. Marrone, and G. Scioscia, Phys. Rev. **D59**, *033001* (1999) .

[25] R. Barate *et al.* (ALEPH Collaboration), CERN-PPE-97-138, (1997).

[26] See, for example, G. Bhattacharyya, Nucl. Phys. (Proc. Suppl.) **52A**, 83 (1997); V. Bednyakov, A. Faessler, and S. Kovalenko, hep-ph/9904414.

[27] T. Falk and K. Olive, Phys. Lett. **B439**, 71 (1998).

Table caption :

Table 1 — Numerical 1-loop neutron EDM results from SUSY without R parity, for four illustrative cases. All EDM numbers are in $e\,$cm. Note that the quark EDM numbers are direct output from the numerical program applying our quark dipole formulae; while the neutron EDM numbers are from the valence quark model formula, as given in Eq.(1). R-parity violating parameters not given are taken as essentially zero. All parameters are taken real except those with complex phases explicitly listed in each case, where the real number(s) listed then give the magnitude(s). Parameter A here means a common A_u and A_d. Only M_2 is shown for the gaugino masses; the others are fixed by the unification relationship. Explicitly, we use $M_1 = 0.5\,M_2$ and $M_3 = 3.5\,M_2$. The first column under "EDM Results" gives the couplings of the loop vertices involved. A g indicates either one of the electroweak gauge couplings, while a λ' coupling means one with the appropriate admissible flavor indices. In the explicit results of the four cases, the latter is always a λ'_{311}. The second column gives the reference Feynman diagram figures, when available. The third column indicates whether the particular contribution involves a LR squark mixing. In the case that the mixing is involved and a R-parity violating (RPV) one is involved in generating a RPV EDM contribution, it is marked with "RPV".

Figure captions :

Fig. 1 — Diagram for d-quark EDM from the gaugino loop.

Fig. 2 — Diagrams with neutral gaugino-Higgsino mixing for d-quark EDM.

Fig. 3 — R-parity violating neutralinolike loop diagrams for d-quark EDM. Naive electroweak-state analysis suggests that such a diagram is proportional to a vanishing l^0_k-gaugino mass mixing.

Fig. 4 — Diagram for d-quark EDM suggesting involvement of Majorana masses among the l^0_α or "neutrinos".

Fig. 5 — Diagrams for u- and d-quark EDMs with charged gaugino-Higgsino mixing.

Fig. 6 — R-parity violating charginolike loop diagram for d-quark EDM. Naive electroweak-state analysis suggests that the diagram is proportional to the vanishing l^-_k–$\tilde{W}^+$ mass term.

Fig. 7 — Diagrams for u- and d-quark EDMs with a μ_α mass insertion.

Fig. 8 — Diagrams for u- and d-quark EDMs with a B_α scalar mass insertion.

Fig. 9 — Diagrams with a Majorana-like scalar mass insertion for u- and d-quark EDMs. For the u-quark case, the direct Majorana-like h_u mass insertion is explicitly shown. For

the d-quark case, the corresponding direct h_d mass insertion is obvious, for $\alpha = \beta = 0$; for α and/or β nonzero, the naive direct result from the diagram would vanish, due to the vanishing VEVs.

Fig. 10 — Logarithmic plot of (the magnitude of) the RPV neutron EDM result for μ_0 value between $\pm 2000\,\mathrm{GeV}$, with the other parameters set at the same values as case A in Table 1. The lines marked by G, C, N, and "Total" give the complete gluino, charginolike, neutralinolike, and total (*i.e.,* sum of the three) contributions, respectively. Note that the values of the N contributions and those of the C line for $\mu_0 < -900\,\mathrm{GeV}$ are negative.

Fig. 11 — Logarithmic plot of (the magnitude of) the neutron EDM result verses $\tan\beta$. We show here the MSSM result, our general result with the RPV phase only, and the generic result with complex phases of both kinds. In particular, the A and μ_0 phases are chosen as 7^o and 0.1^o respectively, for the MSSM line. They are zero for the RPV-only line, with which we have a phase of $\frac{\pi}{4}$ for λ'_{311}. All the given nonzero values are used for the three phases for the generic result (from our complete formulae) marked by "GSSM". Again, the other unspecified input parameters are the same as for case A of Table 1.

Fig. 12 — Logarithmic plot of (the magnitude of) the neutron EDM result versus θ_A (the complex phase for the A parameter). The four lines shown are characterized by the $\tan\beta$ values (3 or 50) used and whether it is for our GSSM result (again with a phase of $\frac{\pi}{4}$ for λ'_{311}) — marked by G; or the result for MSSM — marked by M. Again, the λ'_{311} phase is set at $\frac{\pi}{4}$ for the G lines, and the μ_0 phase at 0.1^o for all; the other unspecified input parameters are the same as for case A of Table 1.

Fig. 13 — Logarithmic plot of (the magnitude of) the neutron EDM result verses M_2. The four lines correspond to the four cases of Fig. 12, each with θ_A set at the dip location, *i.e.,* G-3 for GSSM at $\tan\beta = 3$ with $\theta_A = 2^o$, M-3 for MSSM at $\tan\beta = 3$ with $\theta_A = -1^o$, G-50 for GSSM at $\tan\beta = 50$ with $\theta_A = 20^o$, M-50 for MSSM at $\tan\beta = 50$ with $\theta_A = 3^o$. All other unspecified input parameters are the same as for Fig. 12.

Choice of Parameters

$\tilde{m}_Q = 300\,\text{GeV}$, $\tilde{m}_u = \tilde{m}_d = 200\,\text{GeV}$, $A = M_2 = 300\,\text{GeV}$, $\mu_0 = -300\,\text{GeV}$

$\tan\beta$		3	3	3	50
μ_3		$1 \cdot 10^{-3}\,\text{GeV}$	$1\,\text{GeV}$	$1\,\text{GeV}$	$5 \cdot 10^{-3}\,\text{GeV}$
λ'_{311}		0.05	0.05	0.05	0.05
(complex phases)		$\lambda'_{311}(\pi/4)$	$\lambda'_{311}(\pi/4)$	$\mu_0(0.5^o)$, $A(10^o)$	$\mu_0(0.02^o)$, $\mu_3(-\pi/4)$

EDM RESULTS :-

couplings	Fig.	LR mixing	Case A	Case B	Case C	Case D
d quark EDM						
Gluino loop : -						
α_s	1	RPV	$8.8 \cdot 10^{-28}$	$8.8 \cdot 10^{-25}$	$-3.9 \cdot 10^{-26}$	$-6.7 \cdot 10^{-29}$
Neutralino-like loop : -						
g^2	1	RPV	$-1.9 \cdot 10^{-29}$	$-1.9 \cdot 10^{-26}$	$8.3 \cdot 10^{-28}$	$2.7 \cdot 10^{-30}$
$g \cdot y_d$	2	no	~ 0	~ 0	$-1.6 \cdot 10^{-27}$	$-1.2 \cdot 10^{-27}$
$g \cdot \lambda'_{i11}$	3	no	$-1.0 \cdot 10^{-28}$	$-1.0 \cdot 10^{-25}$	$1.1 \cdot 10^{-27}$	$1.1 \cdot 10^{-27}$
y_d^2	4	RPV	$9.7 \cdot 10^{-37}$	$9.7 \cdot 10^{-34}$	$-3.9 \cdot 10^{-35}$	$-2.6 \cdot 10^{-33}$
$y_d \cdot \lambda'_{ijk}$	4	yes	$-1.7 \cdot 10^{-36}$	$-1.7 \cdot 10^{-33}$	$8.5 \cdot 10^{-35}$	$2.5 \cdot 10^{-33}$
two λ'_{ijk}	4	yes	$-2.1 \cdot 10^{-39}$	$-3.4 \cdot 10^{-34}$	$9.0 \cdot 10^{-35}$	$-8.6 \cdot 10^{-37}$
Chargino-like loop : -						
$g \cdot y_d$	5	no	~ 0	0	$2.5 \cdot 10^{-26}$	$1.7 \cdot 10^{-26}$
$g \cdot \lambda'_{i11}$	6	no	$2.1 \cdot 10^{-27}$	$2.1 \cdot 10^{-24}$	$-1.3 \cdot 10^{-26}$	$-1.7 \cdot 10^{-26}$
$y_u \cdot y_d$	7	yes	~ 0	0	$-2.7 \cdot 10^{-34}$	$-8.0 \cdot 10^{-36}$
$y_u \cdot \lambda'_{ijk}$	7	yes	$-2.1 \cdot 10^{-37}$	$-2.1 \cdot 10^{-33}$	$3.8 \cdot 10^{-34}$	$8.3 \cdot 10^{-36}$
u quark EDM						
Gluino loop : -						
α_s	1	yes	0	0	$4.5 \cdot 10^{-26}$	$-1.8 \cdot 10^{-30}$
Neutralinolike loop : -						
g^2	1	yes	~ 0	0	$2.6 \cdot 10^{-27}$	$-1.4 \cdot 10^{-31}$
$g \cdot y_u$	2	no	~ 0	0	$2.1 \cdot 10^{-28}$	$5.3 \cdot 10^{-31}$
y_u^2	4	yes	~ 0	0	$1.3 \cdot 10^{-37}$	$4.0 \cdot 10^{-41}$
Charginolike loop : -						
$g \cdot y_u$	5	no	~ 0	~ 0	$-1.3 \cdot 10^{-27}$	$-3.2 \cdot 10^{-30}$
$y_u \cdot y_d$	7	RPV	$-7.6 \cdot 10^{-36}$	$-7.6 \cdot 10^{-33}$	$3.2 \cdot 10^{-34}$	$6.4 \cdot 10^{-34}$
$y_u \cdot \lambda'_{ijk}$	7	RPV	$9.7 \cdot 10^{-36}$	$9.7 \cdot 10^{-33}$	$-5.1 \cdot 10^{-34}$	$-6.4 \cdot 10^{-34}$
Neutron EDM						
from Gluino loop :			$1.8 \cdot 10^{-27}$	$1.8 \cdot 10^{-24}$	$-1.0 \cdot 10^{-25}$	$-1.4 \cdot 10^{-28}$
from Charginolike loop :			$4.3 \cdot 10^{-27}$	$4.3 \cdot 10^{-24}$	$2.5 \cdot 10^{-26}$	$2.4 \cdot 10^{-28}$
from Neutralinolike loop :			$-2.9 \cdot 10^{-28}$	$-2.9 \cdot 10^{-25}$	$-8.6 \cdot 10^{-28}$	$-2.0 \cdot 10^{-29}$
TOTAL :			$5.8 \cdot 10^{-27}$	$5.8 \cdot 10^{-24}$	$-7.8 \cdot 10^{-26}$	$8.0 \cdot 10^{-29}$

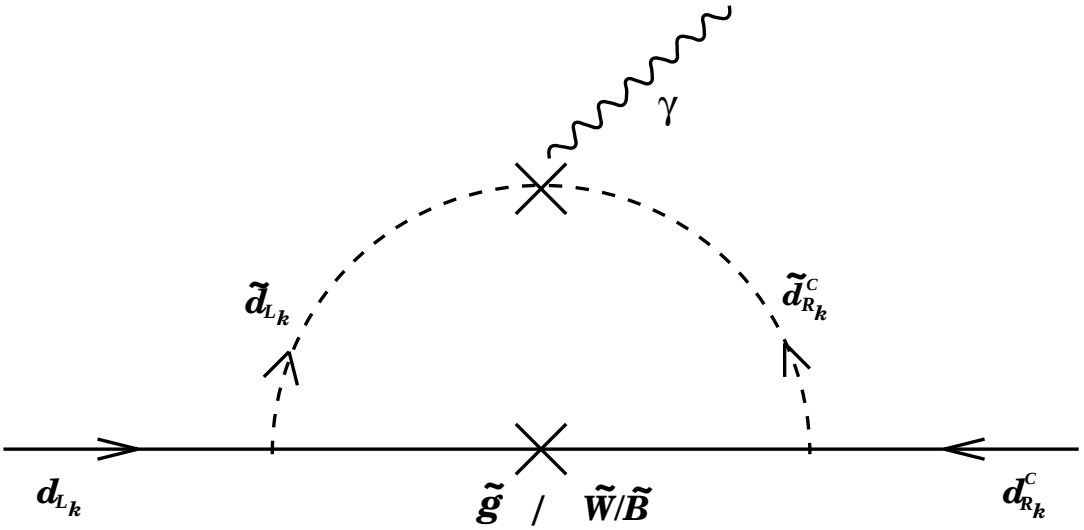

FIG. 1. Diagram for d-quark EDM from the gaugino loop.

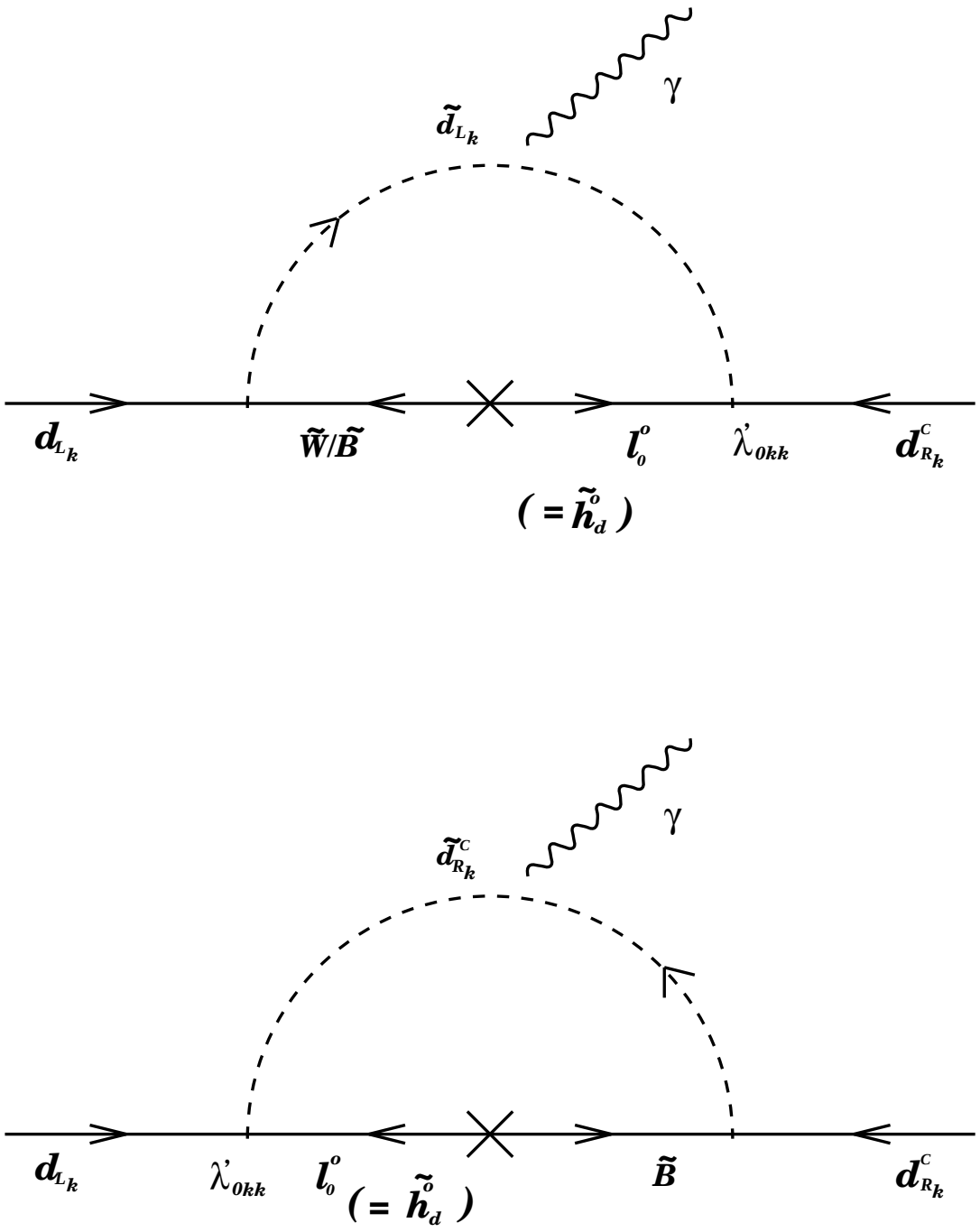

FIG. 2. Diagrams with neutral gaugino-Higgsino mixing for d-quark EDM.

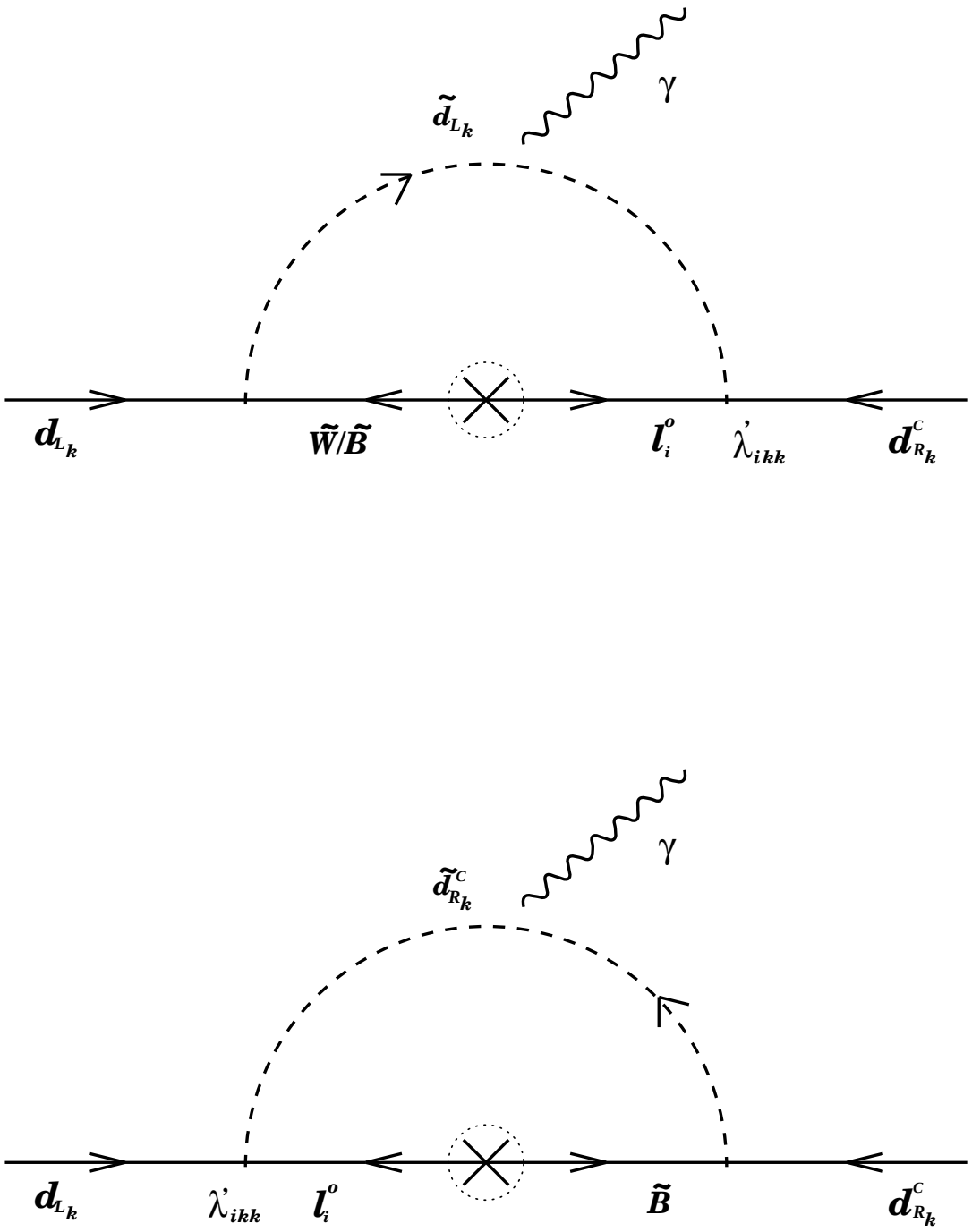

FIG. 3. R-parity violating neutralinolike loop diagrams for d-quark EDM. Naive electroweak-state analysis suggests that such a diagram is proportional to a vanishing l_k^0-gaugino mass mixing.

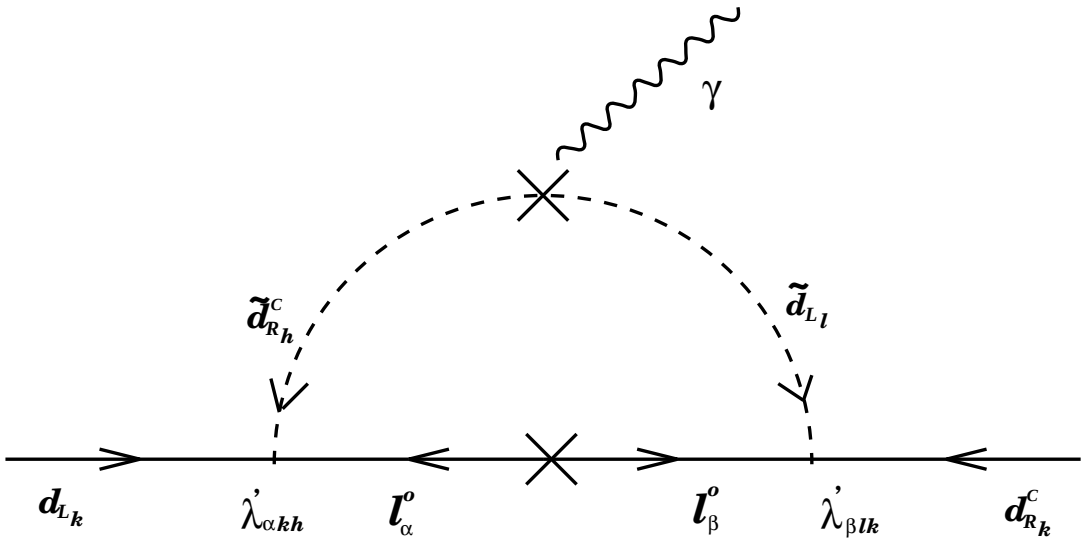

FIG. 4. Diagram for d-quark EDM suggesting involvement of Majorana masses among the l^0_α or "neutrinos".

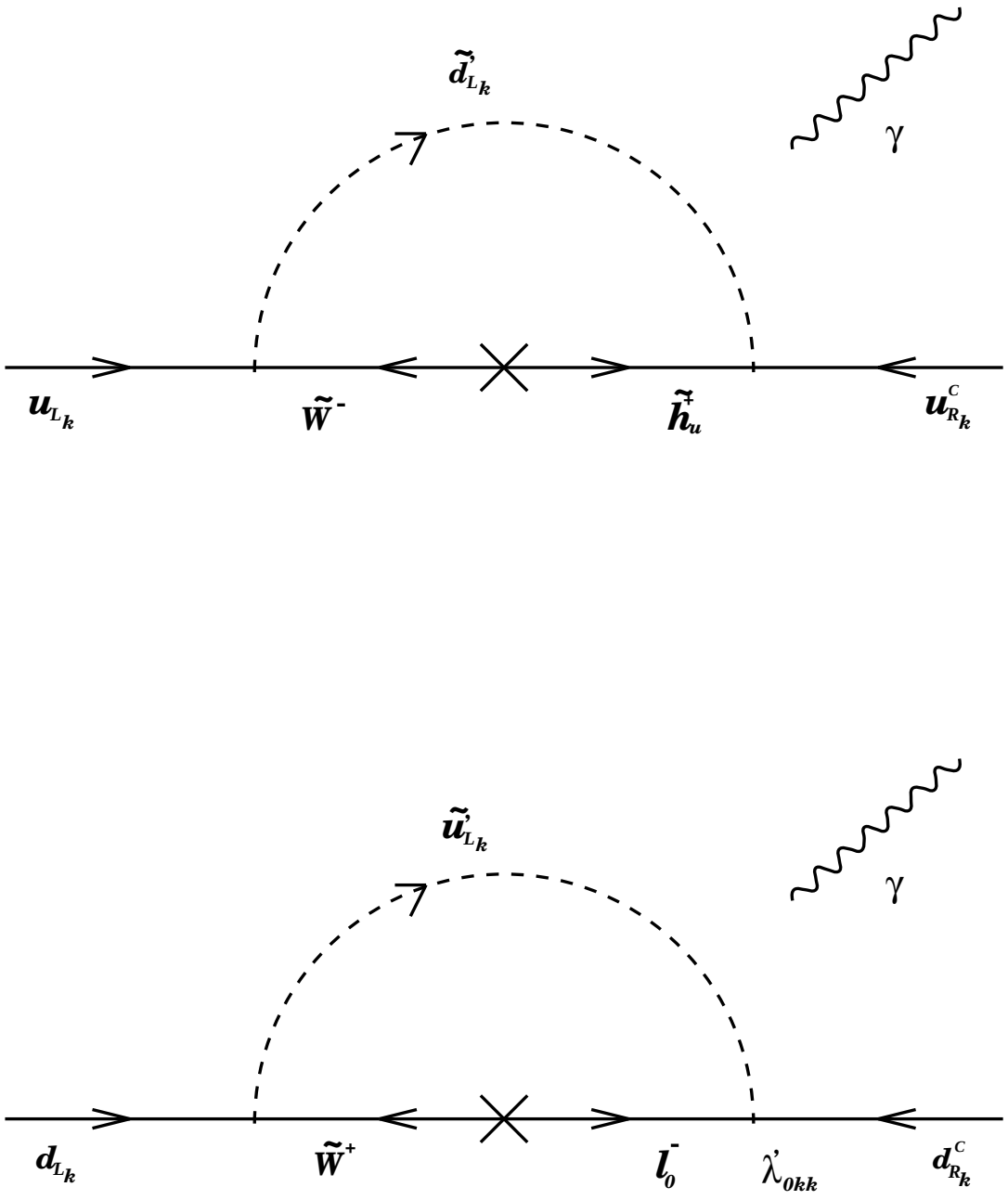

FIG. 5. Diagrams for u- and d-quark EDMs with charged gaugino-Higgsino mixing.

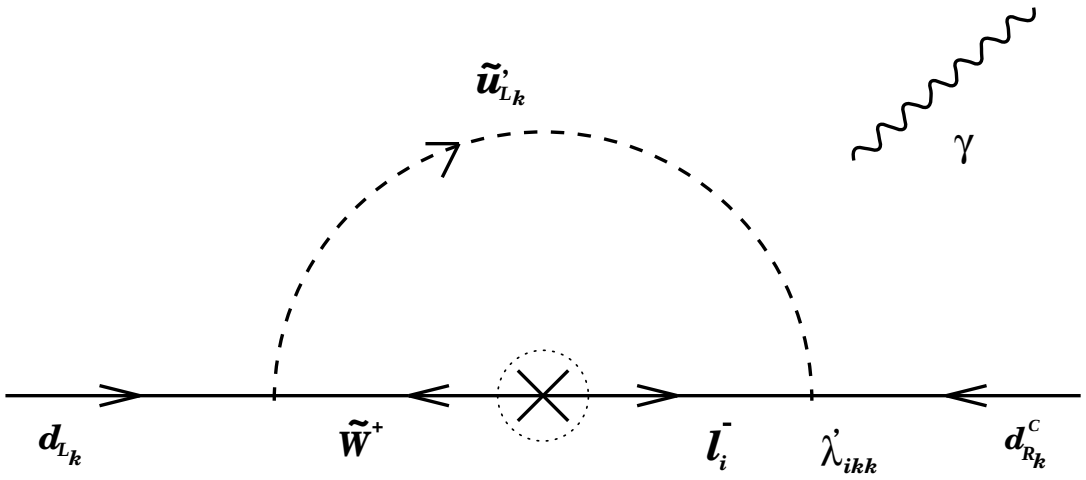

FIG. 6. R-parity violating charginolike loop diagram for d-quark EDM. Naive electroweak-state analysis suggests that the diagram is proportional to the vanishing l_k^-–$\tilde{W}^+$ mass term.

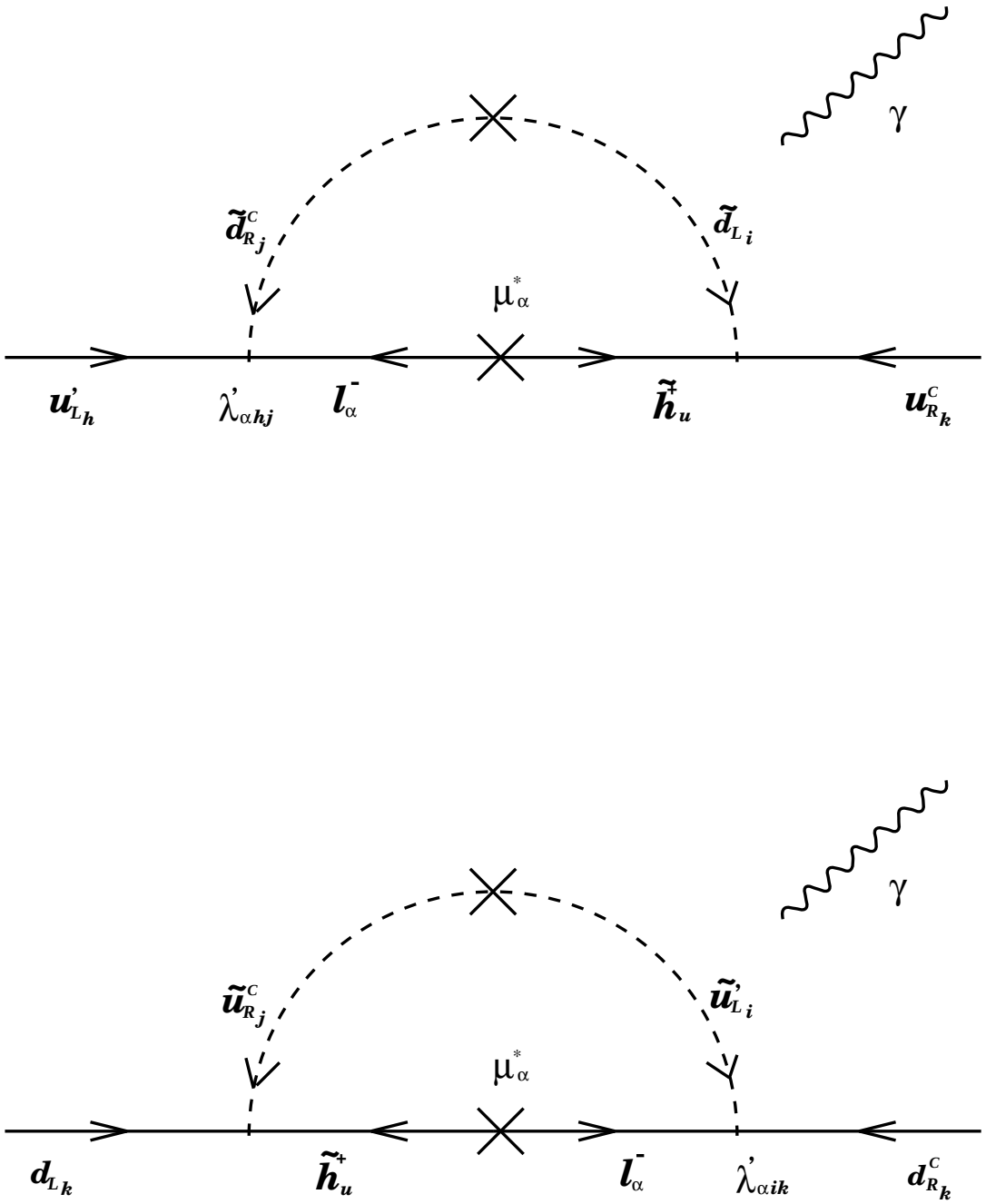

FIG. 7. Diagrams for u- and d-quark EDMs with a μ_α mass insertion.

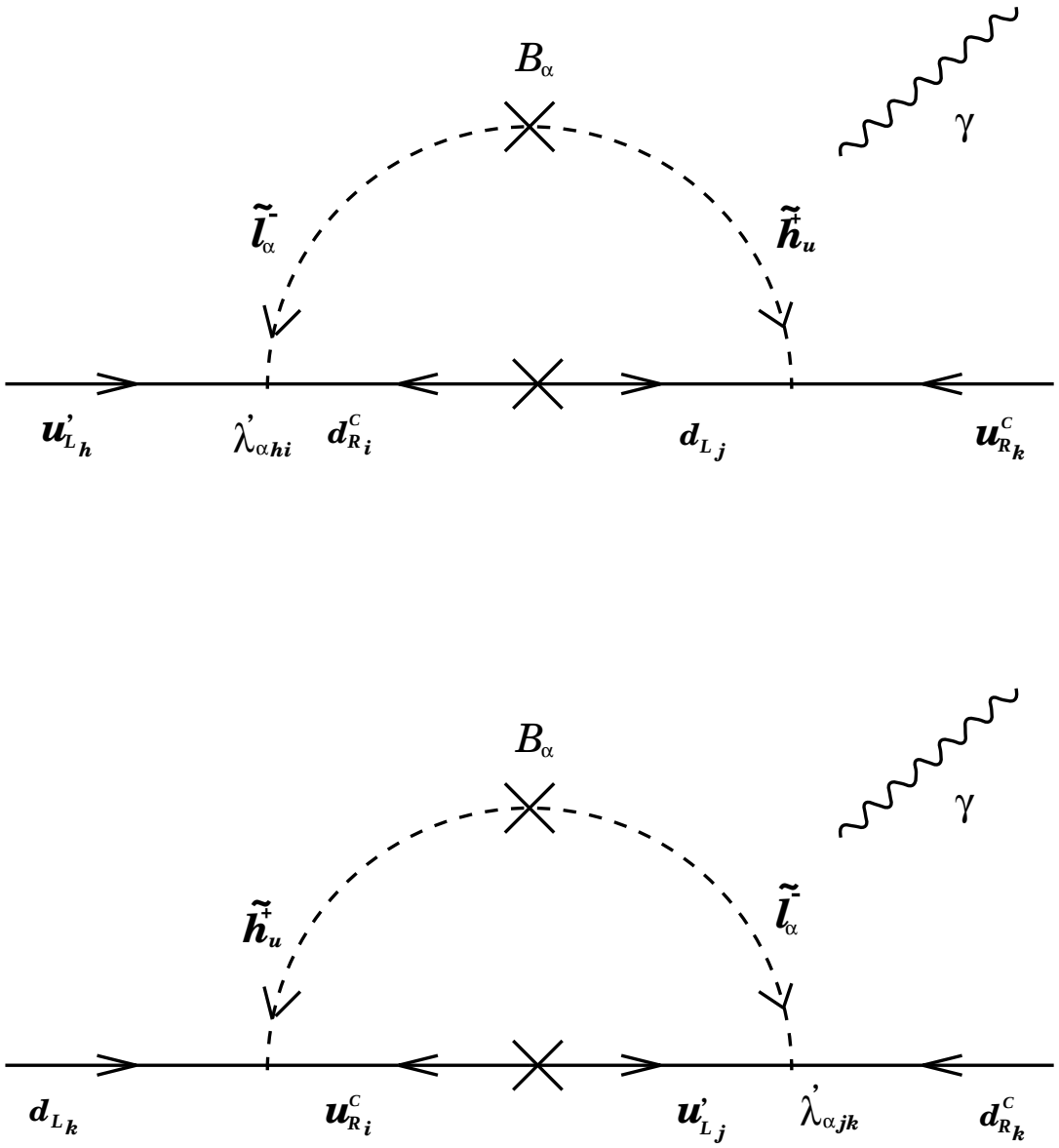

FIG. 8. Diagrams for u- and d-quark EDMs with a B_α scalar mass insertion.

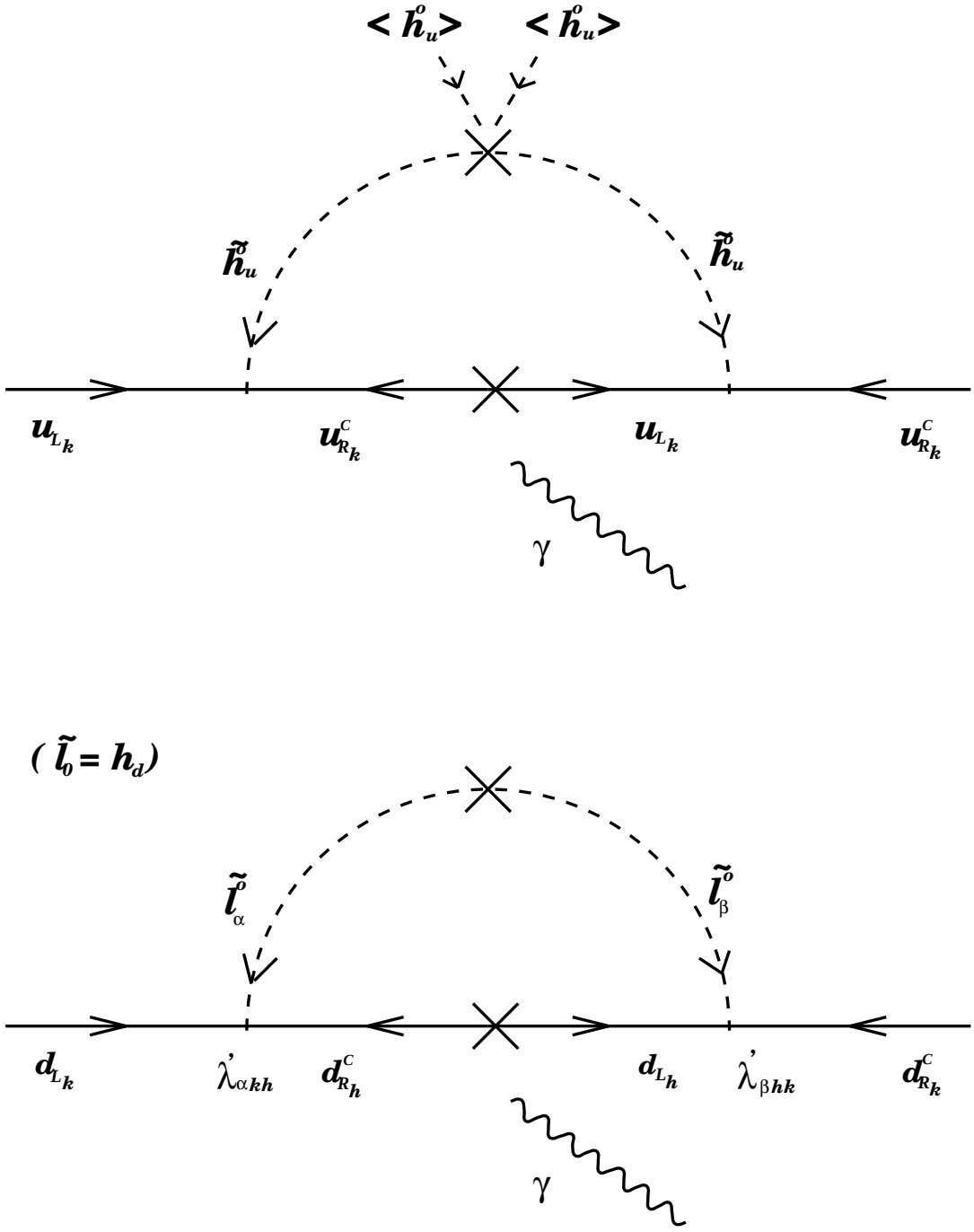

FIG. 9. Diagrams with a Majorana-like scalar mass insertion for u- and d-quark EDMs. For the u-quark case, the direct Majorana-like h_u mass insertion is explicitly shown. For the d-quark case, the corresponding direct h_d mass insertion is obvious, for $\alpha = \beta = 0$; for α and/or β nonzero, the naive direct result from the diagram would vanish, due to the vanishing VEVs.

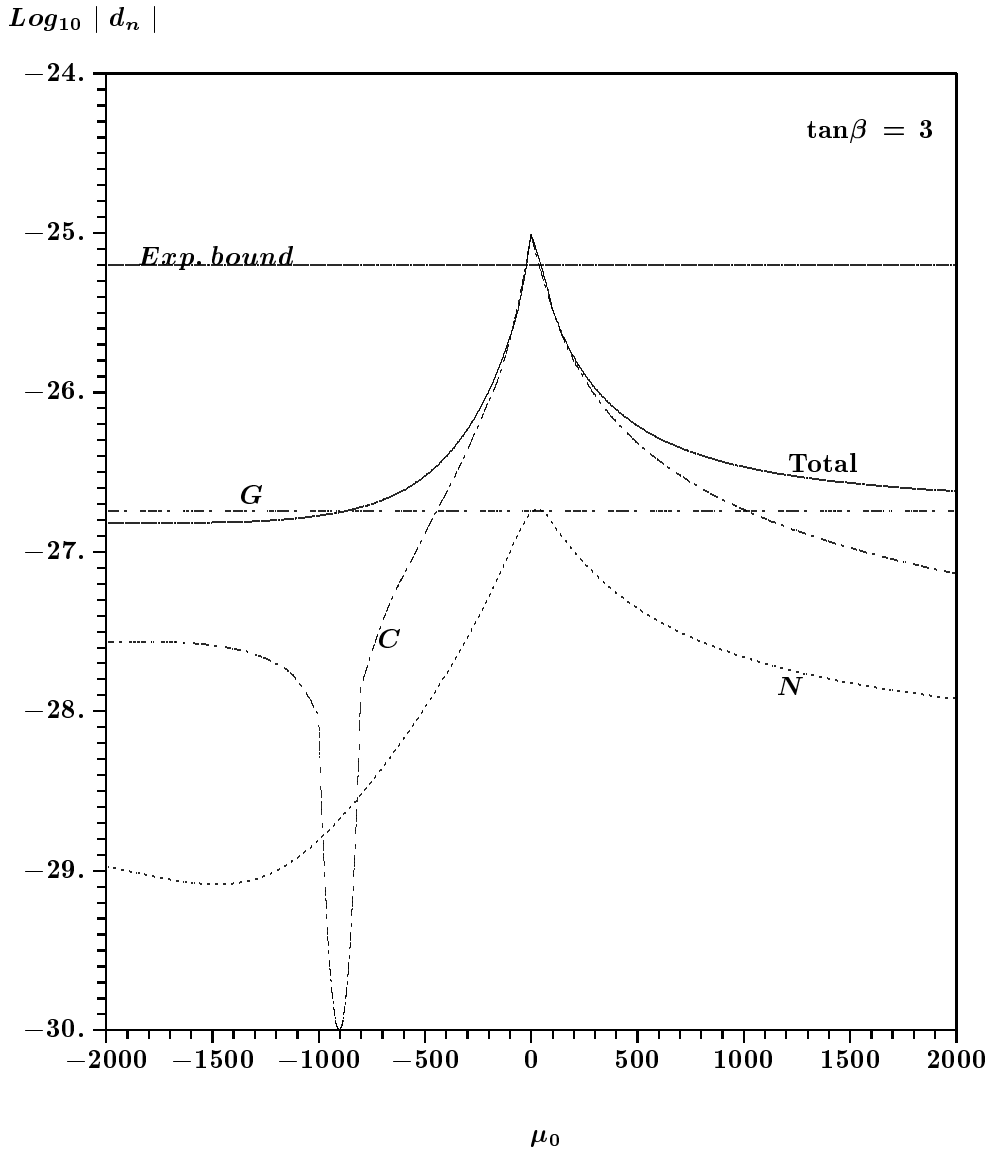

FIG. 10. Logarithmic plot of (the magnitude of) the RPV neutron EDM result for μ_0 value between $\pm 2000\,\mathrm{GeV}$, with the other parameters set at the same values as case A in Table 1. The lines marked by G, C, N, and "Total" give the complete gluino, charginolike, neutralinolike, and total (*i.e.,* sum of the three) contributions, respectively. Note that the values of the N contributions and those of the C line for $\mu_0 < -900\,\mathrm{GeV}$ are negative.

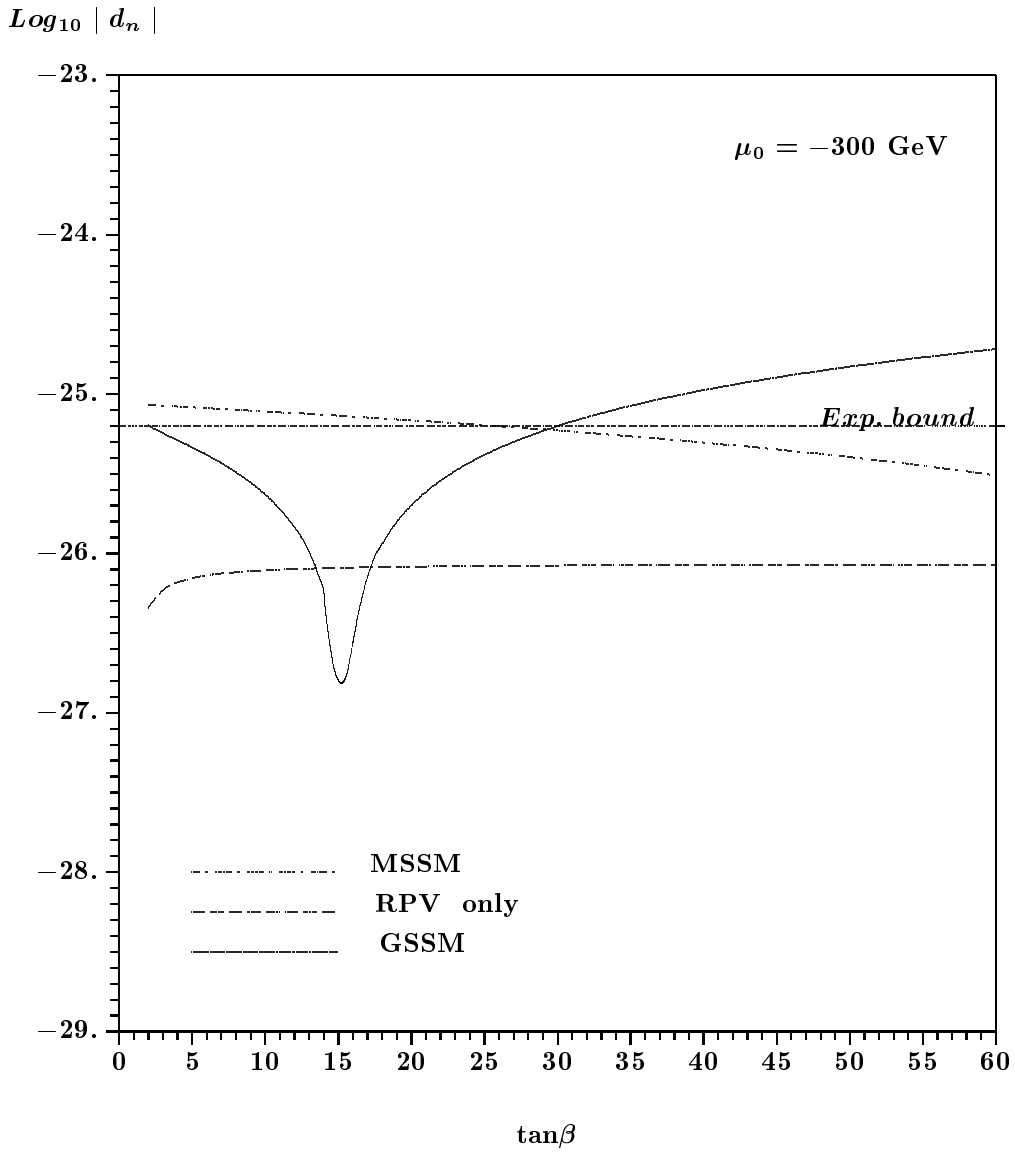

FIG. 11. Logarithmic plot of (the magnitude of) the neutron EDM result verses tanβ. We show here the MSSM result, our general result with the RPV phase only, and the generic result with complex phases of both kinds. In particular, the A and μ_0 phases are chosen as 7^o and 0.1^o respectively, for the MSSM line. They are zero for the RPV-only line, with which we have a phase of $\frac{\pi}{4}$ for λ'_{311}. All the given nonzero values are used for the three phases for the generic result (from our complete formulae) marked by "GSSM". Again, the other unspecified input parameters are the same as for case A of Table 1.

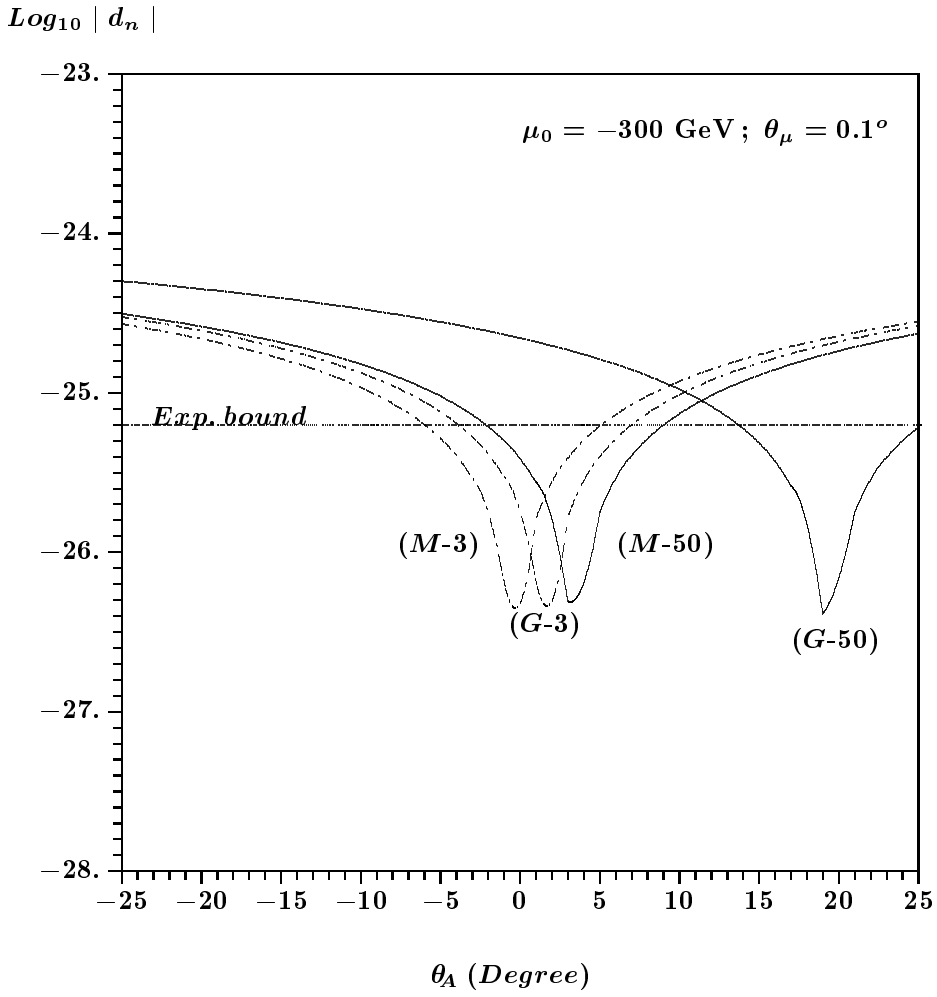

FIG. 12. Logarithmic plot of (the magnitude of) the neutron EDM result versus θ_A (the complex phase for the A parameter). The four lines shown are characterized by the tanβ values (3 or 50) used and whether it is for our GSSM result (again with a phase of $\frac{\pi}{4}$ for $\chi'_{3\text{ll}}$) — marked by G; or the result for MSSM — marked by M. Again, the $\chi'_{3\text{ll}}$ phase is set at $\frac{\pi}{4}$ for the G lines, and the μ_0 phase at 0.1^o for all; the other unspecified input parameters are the same as for case A of Table 1.

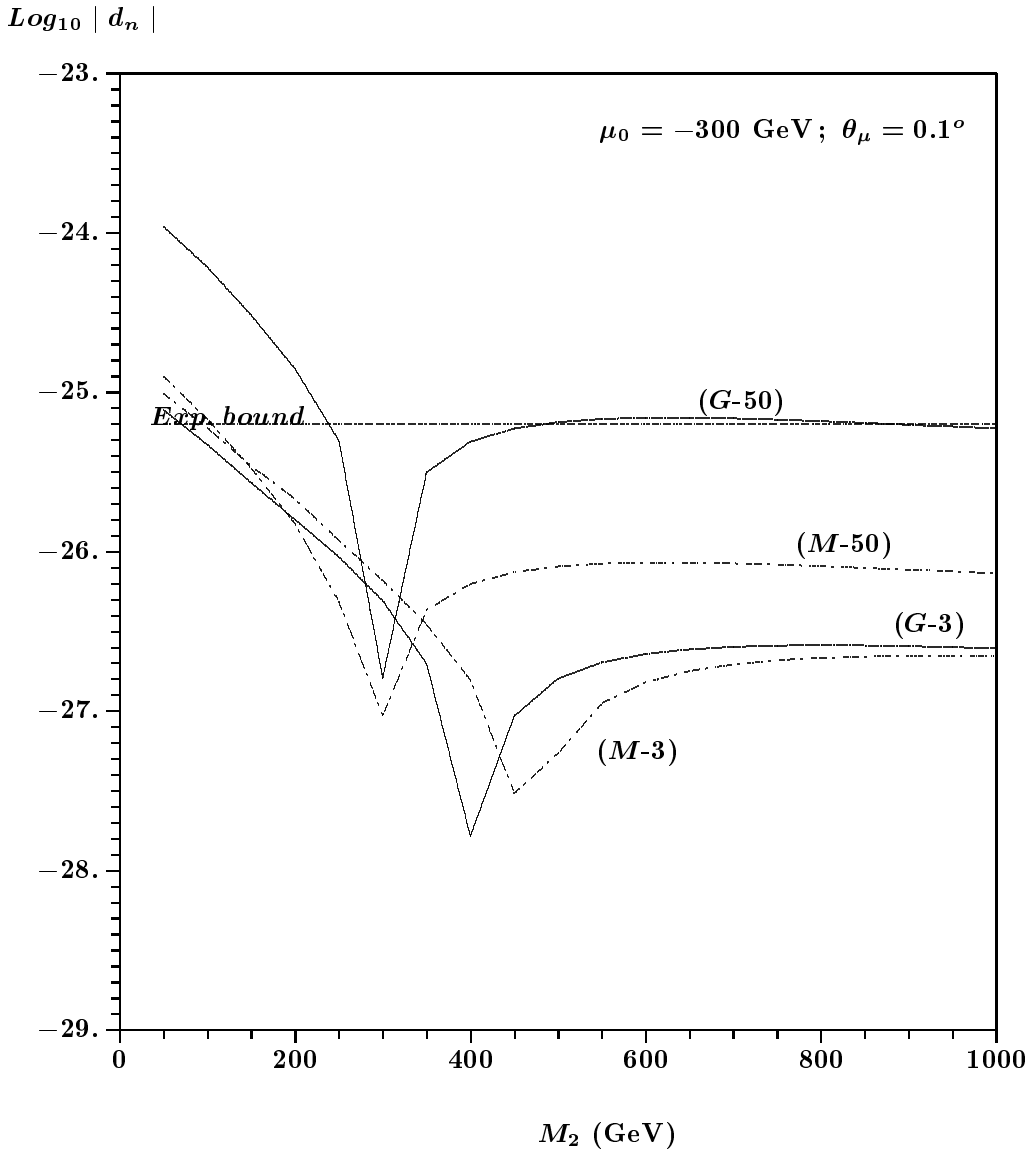

FIG. 13. Logarithmic plot of (the magnitude of) the neutron EDM result versus M_2. The four lines correspond to the four cases of Fig. 12, each with θ_A set at the dip location, *i.e.,* G-3 for GSSM at $\tan\beta = 3$ with $\theta_A = 2^o$, M-3 for MSSM at $\tan\beta = 3$ with $\theta_A = -1^o$, G-50 for GSSM at $\tan\beta = 50$ with $\theta_A = 20^o$, M-50 for MSSM at $\tan\beta = 50$ with $\theta_A = 3^o$. All other unspecified input parameters are the same as for Fig. 12.